TRPC6 is the endothelial calcium channel that regulates leukocyte transendothelial migration during the inflammatory response

Evan W. Weber,[1] Fei Han,[1] Mohammad Tauseef,[2] Lutz Birnbaumer,[3] Dolly Mehta,[2] and William A. Muller[1]

[1]Department of Pathology, Northwestern University Feinberg School of Medicine, Chicago, IL 60611
[2]Department of Pharmacology, Center for Lung and Vascular Biology, University of Illinois in Chicago College of Medicine, Chicago, IL 60612
[3]Neurobiology Laboratory, National Institute of Environmental Health Sciences, Research Triangle Park, NC 27709

Leukocyte transendothelial migration (TEM) is a tightly regulated, multistep process that is critical to the inflammatory response. A transient increase in endothelial cytosolic free calcium ion concentration (↑$[Ca^{2+}]_i$) is required for TEM. However, the mechanism by which endothelial ↑$[Ca^{2+}]_i$ regulates TEM and the channels mediating this ↑$[Ca^{2+}]_i$ are unknown. Buffering ↑$[Ca^{2+}]_i$ in endothelial cells does not affect leukocyte adhesion or locomotion but selectively blocks TEM, suggesting a role for ↑$[Ca^{2+}]_i$ specifically for this step. Transient receptor potential canonical 6 (TRPC6), a Ca^{2+} channel expressed in endothelial cells, colocalizes with platelet/endothelial cell adhesion molecule-1 (PECAM) to surround leukocytes during TEM and clusters when endothelial PECAM is engaged. Expression of dominant-negative TRPC6 or shRNA knockdown in endothelial cells arrests neutrophils apically over the junction, similar to when PECAM is blocked. Selectively activating endothelial TRPC6 rescues TEM during an ongoing PECAM blockade, indicating that TRPC6 functions downstream of PECAM. Furthermore, endothelial TRPC6 is required for trafficking of lateral border recycling compartment membrane, which facilitates TEM. Finally, mice lacking TRPC6 in the nonmyeloid compartment (i.e., endothelium) exhibit a profound defect in neutrophil TEM with no effect on leukocyte trafficking. Our findings identify endothelial TRPC6 as the calcium channel mediating the ↑$[Ca^{2+}]_i$ required for TEM at a step downstream of PECAM homophilic interactions.

CORRESPONDENCE
William A. Muller:
wamuller@northwestern.edu

Abbreviations used: ↑$[Ca^{2+}]_i$, transient increase in endothelial cytosolic free calcium ion concentration; 3D, three dimensional; Ab, antibody; BAPTA-AM, 1,2-Bis(2-aminophenoxy)ethane-N,N,N′,N′-tetraacetic acid tetrakis(acetoxymethyl ester); DAG, diacylglycerol; LBRC, lateral border recycling compartment; MLCK, myosin light chain kinase; OAG, 1-Oleoyl-2-acetyl-*sn*-glycerol; PECAM, platelet/endothelial cell adhesion molecule-1; TEER, transendothelial electrical resistance; TEM, transendothelial migration; TRP, transient receptor potential; VE-cadherin, vascular endothelial cadherin.

During the inflammatory response, leukocytes are recruited into the affected tissue through a series of tightly regulated and mechanistically distinct interactions with the vascular endothelium (Ley et al., 2007; Muller, 2011). The final step, in which leukocytes traverse the endothelium by squeezing between two tightly opposed endothelial cells, is called transendothelial migration (TEM). In contrast to events upstream of TEM (e.g., leukocyte rolling or adhesion), TEM is generally irreversible and is thus considered an ideal target for antiinflammatory therapeutic intervention.

Several endothelial adhesion molecules and their intracellular signaling mechanisms have been demonstrated to regulate TEM (Muller, 2011). One such adhesion molecule is platelet/endothelial cell adhesion molecule-1 (PECAM). PECAM is an immunoglobulin superfamily transmembrane protein localized to endothelial cell–cell borders and expressed diffusely on the surface of leukocytes (Muller, 1992). Homophilic interactions between leukocyte and endothelial PECAM are required for TEM (Muller et al., 1993). Immunological or genetic inhibition of these interactions greatly attenuates TEM both in vitro and in vivo (Muller et al., 1993; Bogen et al., 1994; Berman et al., 1996; Mamdouh et al., 2003; Schenkel et al., 2004; Dasgupta et al., 2010).

PECAM and other adhesion molecules that regulate TEM, like CD99, poliovirus receptor (PVR), and junctional adhesion molecule-A

The Rockefeller University Press $30.00
J. Exp. Med. 2015 Vol. 212 No. 11 1883–1899
www.jem.org/cgi/doi/10.1084/jem.20150353

(JAM-A), partially reside in a unique endothelial organelle called the lateral border recycling compartment (LBRC; Mamdouh et al., 2003, 2009). The LBRC consists of many interconnected 50-nm tubulovesicular membrane structures located beneath the plasma membrane at endothelial borders. During TEM, LBRC membrane traffics to surround the transmigrating leukocyte in a process known as targeted recycling (Mamdouh et al., 2003, 2008, 2009; Dasgupta et al., 2009; Sullivan et al., 2014; Winger et al., 2014). Local enrichment of LBRC provides the transmigrating leukocyte with a pool of unligated adhesion molecules, like PECAM and CD99, as well as additional surface area on which to migrate. Targeted recycling is also believed to help maintain endothelial barrier function during TEM in spite of transient displacement of adherens and tight junction proteins (Winger et al., 2014). Initial leukocyte–endothelial PECAM homophilic interactions and kinesin trafficking along microtubules are required for trafficking of LBRC, as blocking these processes inhibits targeted recycling (Mamdouh et al., 2003, 2008). However, other signaling mechanisms that govern targeted recycling have yet to be elucidated.

In addition to PECAM and targeted recycling, several other endothelial signaling events have been implicated in TEM. A transient increase in endothelial cytosolic free calcium ion concentration (↑$[Ca^{2+}]_i$) is one such signal. Pharmacological chelation of endothelial Ca^{2+} during TEM results in a phenotype in which leukocytes adhere normally to the apical surface of endothelial cells but are unable to transmigrate across (Huang et al., 1993; Etienne-Manneville et al., 2000; Su et al., 2000; Kielbassa-Schnepp et al., 2001; Carman and Springer, 2004). Interestingly, the block in TEM observed upon endothelial Ca^{2+} chelation is phenotypically similar to blocking PECAM homophilic interactions with primary antibody (Ab; Muller et al., 1993), suggesting that these two processes might be related. The effects of endothelial Ca^{2+} chelation have been reproducible in various cell culture systems, but the source of ↑$[Ca^{2+}]_i$, which calcium channels are involved, and other mechanistic details are still unclear.

Endothelial cells express a subclass of transient receptor potential (TRP) ion channels that are activated directly by diacylglycerol (DAG; Hofmann et al., 1999), of which TRP canonical 6 (TRPC6) is the most highly expressed (Paria et al., 2004; Yip et al., 2004). TRPC6 is a nonselective cation channel that is fivefold more permeable to Ca^{2+} than Na^+ (Hofmann et al., 1999; Dietrich et al., 2003; Shi et al., 2004). Endothelial TRPC6 has been demonstrated to play an important role in regulating endothelial permeability in response to various cytokines and inflammatory mediators (Leung et al., 2006; Singh et al., 2007; Sel et al., 2008; Tauseef et al., 2012; Weissmann et al., 2012), but its role during leukocyte–endothelial interactions has not yet been investigated.

In the present study, we demonstrate that TRPC6 is the long-sought calcium channel responsible for the ↑$[Ca^{2+}]_i$ that is required for TEM. TRPC6 functions downstream of PECAM–PECAM interactions to recruit the LBRC during both neutrophil and monocyte TEM. Mice whose endothelial cells are genetically deficient for TRPC6 do not support TEM, wherein neutrophils are arrested on the luminal surface of endothelial cells at the site of inflammation, similar to what is observed in our in vitro model. Collectively, these data highlight a novel and critical role for endothelial TRPC6 during the inflammatory response and provide new insight into PECAM-mediated signaling.

RESULTS

Chelation of cytosolic free Ca^{2+} in endothelial cells attenuates leukocyte TEM

Several laboratories have demonstrated that buffering cytosolic calcium in endothelial cells blocks leukocyte TEM but not leukocyte adhesion to the apical surface of the endothelium (Huang et al., 1993; Etienne-Manneville et al., 2000; Su et al., 2000; Kielbassa-Schnepp et al., 2001; Carman and Springer, 2004). However, the mechanism by which endothelial ↑$[Ca^{2+}]_i$ regulates TEM has not yet been established.

To dissect this signaling pathway, we first verified that we could reproduce previously published results using our standard quantitative endpoint TEM assay. Freshly isolated human leukocytes were incubated with HUVECs cultured on a three-dimensional (3D) collagen matrix and allowed to transmigrate for a specified amount of time (Muller et al., 1993; Lou et al., 2007; Muller and Luscinskas, 2008). Subsequent to fixation and Wright-Giemsa staining, hundreds of leukocytes were scored based on their position relative to the endothelium (i.e., above or below). We determined that loading endothelial cells with at least 20 μM of the calcium chelator 1,2-Bis(2-aminophenoxy)ethane-N,N,N′,N′-tetraacetic acid tetrakis(acetoxymethyl ester) (BAPTA-AM) was enough to effectively buffer the ↑$[Ca^{2+}]_i$ induced by histamine (Fig. 1 a). In agreement with previously published data (Huang et al., 1993; Etienne-Manneville et al., 2000; Su et al., 2000; Kielbassa-Schnepp et al., 2001; Carman and Springer, 2004), pretreating HUVECs with BAPTA-AM attenuated neutrophil (Fig. 1 b) and monocyte (Fig. 1 d) TEM by >50% without affecting apical adhesion (Fig. 1 c). Furthermore, the extent of the TEM blockade by BAPTA was similar to that of anti-PECAM for both neutrophils and monocytes. When BAPTA treatment and anti-PECAM blocking Ab were used simultaneously, an additive blockade in TEM was not observed (Fig. 1, b and d), suggesting that endothelial PECAM signaling and endothelial ↑$[Ca^{2+}]_i$ may be involved in the same signaling pathway that governs TEM.

We next sought to verify that the block in TEM was in fact caused by BAPTA-AM retained in the HUVECs and not a result of residual BAPTA-AM eluting out of the collagen matrix and affecting the leukocytes. HUVEC monolayers were pretreated with BAPTA-AM and then incubated with fresh media for 15 min to simulate the time used in our endpoint TEM assay. The eluate was recovered from these monolayers and used to resuspend neutrophils for the TEM assay. As expected, neutrophils resuspended in BAPTA-AM eluate did not display any defect in TEM (Fig. 1 e), indicating that our observed TEM-blocking phenotype is indeed caused

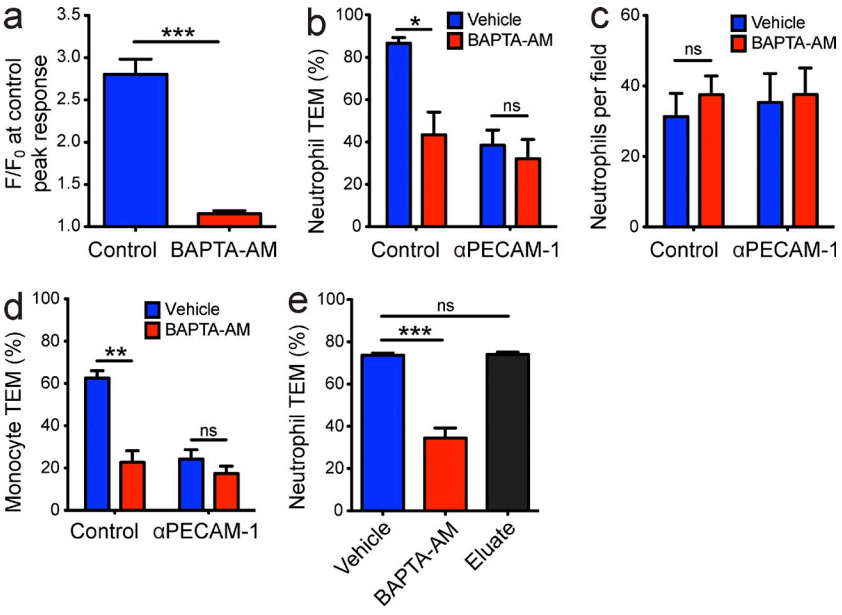

Figure 1. Chelation of cytosolic free Ca^{2+} in endothelial cells attenuates leukocyte TEM. (a) HUVECs were simultaneously loaded with 2.5 µM Fura-2-AM and either 20 µM BAPTA-AM or vehicle (DMSO). Changes in intracellular Ca^{2+} concentration in response to 10 µM histamine were quantified as described in Materials and methods. The plot displays mean ± SEM of the fluorescence/baseline fluorescence (F/F_0) of three independent experiments. At least 100 total cells were individually quantified for each condition. (b–d) Freshly isolated human neutrophils (b and c) or monocytes (d) in the presence or absence of anti-PECAM were added to HUVECs that were pretreated with 20 µM BAPTA-AM or vehicle. (e) Eluate control experiments were performed as previously described (Mamdouh et al., 2008). In brief, BAPTA-AM eluate collected from BAPTA-AM–treated HUVECs was used to resuspend neutrophils, and their ability to transmigrate was subsequently assessed. (b–e) Data represent the mean ± SEM of at least three independent experiments in which each condition was tested in triplicate. *, $P < 0.05$; **, $P < 0.01$; ***, $P < 0.001$ (one- or two-way ANOVA).

by BAPTA-AM that is retained in the HUVECs and not by effects on the leukocyte.

Endothelial ↑$[Ca^{2+}]_i$ is required for LBRC targeted recycling

Because PECAM interactions and ↑$[Ca^{2+}]_i$ appear to act in the same signaling pathway, we hypothesized that endothelial ↑$[Ca^{2+}]_i$ might be downstream of PECAM signaling. To address this question, we performed our standard targeted recycling assay (Mamdouh et al., 2003, 2008, 2009). To avoid bias in our interpretation, all leukocytes in contact with the endothelium were examined, not just the ones that appeared to be undergoing TEM. In control HUVECs, 60–70% of adherent leukocytes were surrounded by LBRC membrane, signifying that targeted recycling had occurred. In contrast, HUVEC pretreatment with BAPTA-AM impaired targeted recycling by ∼50% for neutrophils (Fig. 2, a and b) and ∼70% for monocytes (Fig. 2 e). Leukocytes that were arrested as a result of endothelial BAPTA-AM loading displayed a phenotype similar to that of anti-PECAM blockade, in that they were apically adherent at endothelial junctions (Fig. 2, c and d) but were unable to transmigrate across (Fig. 2 a). These results suggest that ↑$[Ca^{2+}]_i$ is downstream of endothelial PECAM signaling during leukocyte TEM and is required for LBRC targeted recycling.

TRPC6 colocalizes with PECAM at endothelial cell–cell borders and is recruited with PECAM to anti-PECAM–coated polystyrene beads

TRPC6 is a ubiquitously expressed, nonselective, tetrameric cation channel that is fivefold more permeable to Ca^{2+} than Na^+ (Hofmann et al., 1999; Dietrich and Gudermann, 2007). Unlike other Ca^{2+} channels, TRPC6 and isoforms TRPC3 and 7 are activated directly by DAG in a receptor-operated fashion (Hofmann et al., 1999). In endothelial cells, TRPC6 has been implicated in various inflammatory signaling pathways, including thrombin- and bradykinin receptor–induced decreases in endothelial barrier integrity and TLR4 signaling (Leung et al., 2006; Singh et al., 2007; Sel et al., 2008; Tauseef et al., 2012; Weissmann et al., 2012). Many pathways that govern endothelial permeability intersect with those that govern TEM. Thus, we hypothesized that TRPC6 may be the channel regulating ↑$[Ca^{2+}]_i$ during TEM.

We attempted to determine the localization of endogenous TRPC6 by immunofluorescence; however, none of the several anti-TRPC6 Abs we could find were suitable for immunofluorescence. Despite robust staining on Western blots, they either did not stain or produced high background and artifactual staining in endothelial cells (not depicted). We circumvented this problem by expressing tagged versions of TRPC6 to determine its cellular distribution, similar to other groups (Cayouette et al., 2004; Reiser et al., 2005; Fleming et al., 2007; Möller et al., 2007; Horinouchi et al., 2012; Liu et al., 2012; Thilo et al., 2012a; Lei et al., 2014). HUVECs expressing mCherry-tagged TRPC6 were used to determine localization of the channel both at rest and during leukocyte TEM. Fig. 3 a demonstrates strong junctional localization of TRPC6, similar to many other proteins that are relevant to TEM (e.g., PECAM, CD99, JAM-A, and PVR). The presence of perinuclear TRPC6-mCherry in these images may be caused by incomplete processing of exogenous protein in the endoplasmic reticulum or protein trapped in endo- or exocytic recycling vesicles (Lei et al., 2014). Interestingly, during TEM, endothelial TRPC6 colocalizes with PECAM and surrounds transmigrating monocytes (Fig. 3 b) and neutrophils (not depicted). This is in stark contrast to proteins that comprise the adherens and tight junctions, which instead separate to form a gap at the site of TEM (Allport et al., 2000; Shaw et al., 2001; Su et al., 2002; Winger et al., 2014).

During TEM, adhesion molecules expressed on the endothelial surface, like PECAM and CD99, participate in

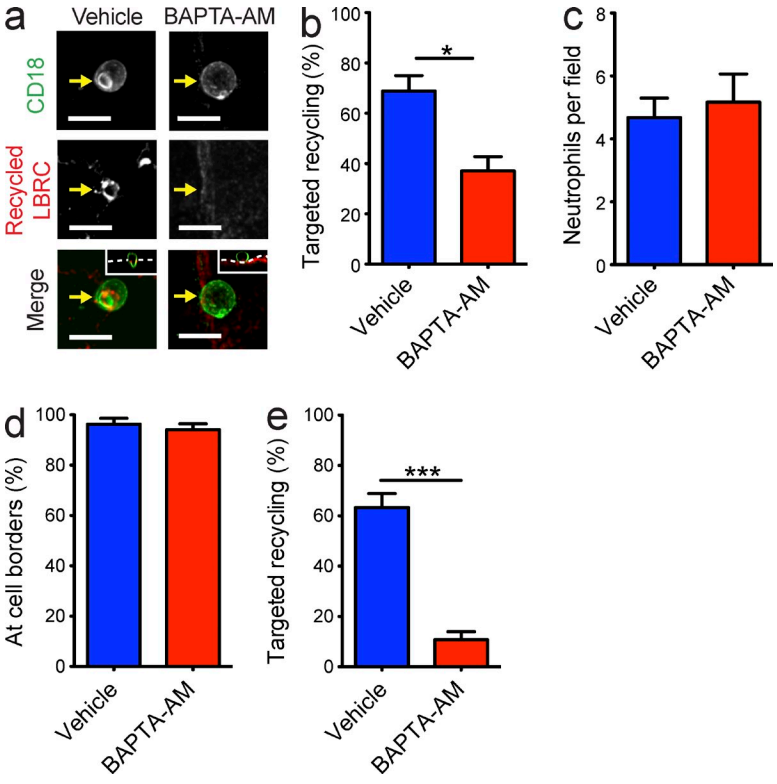

Figure 2. Endothelial ↑$[Ca^{2+}]_i$ is required for LBRC targeted recycling. (a–e) Freshly isolated neutrophils (a–d) or monocytes (e) were added to HUVEC monolayers that were pretreated with vehicle (DMSO) or 20 µM BAPTA-AM. LBRC trafficking (a, b, and e), neutrophil adhesion (c), and neutrophil crawling (d) were assessed using our targeted recycling assay, as described in Materials and methods. Representative images (a) demonstrate targeted recycling to the site of neutrophil TEM (bars, 10 µm). Arrows denote the site where LBRC is or should be enriched. Insets in a are orthogonal (XZ) projections of the arrested neutrophil with respect to the endothelial monolayer (dashed line at the position shown in the merged images). Data represent the mean ± SEM of at least three independent experiments in which each condition was tested in triplicate. *, $P < 0.05$; ***, $P < 0.001$ (Student's *t* test).

homophilic interactions with their cognate receptor molecules on leukocytes (Muller, 2011). These interactions and their resulting signaling components are not global, but rather spatially restricted to areas around the leukocyte. Furthermore, these interactions are required for TEM and targeted recycling (Muller, 2011).

Although PECAM and TRPC6 colocalize at the junction and around transmigrating leukocytes, it was unclear whether this colocalization was functionally or physiologically relevant. To more closely examine the spatial relationship between PECAM and TRPC6, we used an assay in which PECAM Ab–coated polystyrene beads were allowed to interact with the endothelium, much like leukocytes do during TEM. As in a previous study, the coated beads provided high concentrations of a given ligand to the endothelial surface and allowed for identification and analysis of molecules recruited to the area around the bead independent of other molecules that might be expressed or secreted by the leukocyte (Sullivan et al., 2013).

As expected, after 20 min, ∼50% of all anti-PECAM–coated beads recruited endothelial PECAM to concentrate at the bead perimeter and ∼35% of anti-PECAM beads also recruited endothelial TRPC6 (Fig. 3, c and d). Because the timing of this assay was optimized for PECAM recruitment, we expected to observe PECAM recruited at a higher percentage compared with other proteins. Temporal differences in protein recruitment may account for the small gap between PECAM and TRPC6 recruitment percentage. Importantly, nearly all of the anti-PECAM beads that recruited TRPC6 also recruited PECAM (not depicted). The recruitment of TRPC6 to beads coated with PECAM Ab was specific because beads coated with Abs against nonimmune mouse IgG, MHC class I (MHC I), and ICAM-1 recruited neither PECAM nor TRPC6 (Fig. 3, c and d). Anti-PECAM beads failed to recruit vascular endothelial cadherin (VE-cadherin) away from the junction (Fig. 3 c), nor did they recruit CD99, CD47, or intercellular adhesion molecule-1 (ICAM-1; Fig. 3, e and f). These data indicate that recruitment to anti-PECAM beads may be specific to TRPC6, as other endothelial surface molecules known to surround transmigrating leukocytes were not recruited. These data further implicate TRPC6 as a potentially relevant Ca^{2+} channel during TEM and highlight a unique signaling event in which PECAM homophilic interactions lead to recruitment and enrichment of TRPC6.

Activation of endothelial TRPC6 is sufficient to rescue TEM and targeted recycling in neutrophils blocked by anti-PECAM Ab

Based on the data presented thus far, we speculated that endothelial ↑$[Ca^{2+}]_i$ during TEM may be mediated by TRPC6 at a step downstream of leukocyte–endothelial PECAM homophilic interactions. If this were the case, we might expect to overcome a block in TEM imposed by anti-PECAM Ab by activating a step distal to the PECAM-regulated step. To more specifically address this question, we devised an experiment in which neutrophil TEM was first blocked by anti-PECAM Ab. We then added 10 µM of DAG analogue and TRPC6 agonist 1-Oleoyl-2-acetyl-*sn*-glycerol (OAG) or vehicle control (DMSO) to the monolayers to test whether

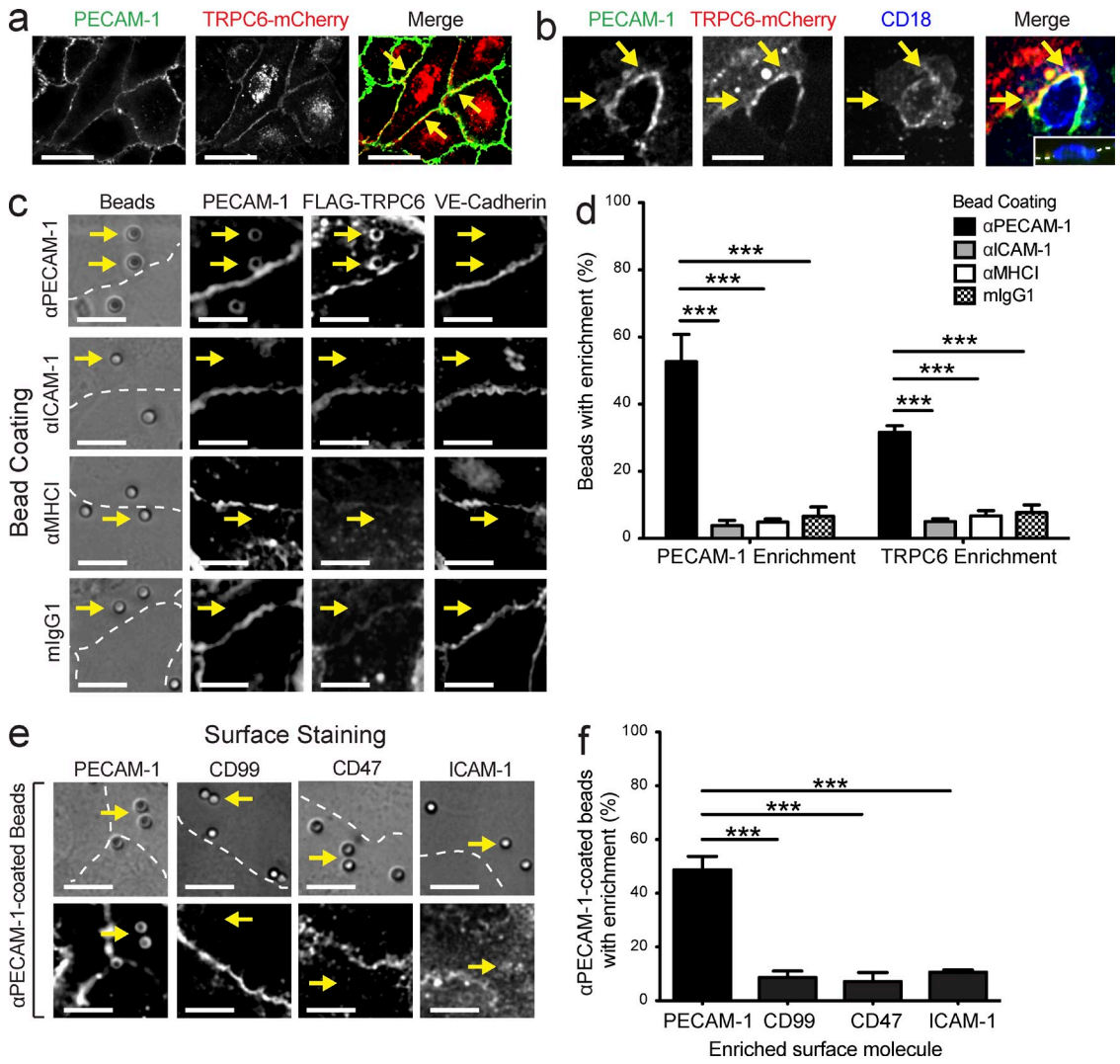

Figure 3. TRPC6 colocalizes with PECAM at endothelial cell–cell borders and is recruited with PECAM to anti–PECAM–coated polystyrene beads. (a and b) HUVECs were transduced with adenovirus expressing mCherry-tagged TRPC6 for 72 h. Monolayers were then immunostained with anti-PECAM (a) and anti-CD18 (b) and subsequently examined by confocal microscopy. Arrows denote sites in which PECAM and TRPC6 are colocalized. The inset in b is an orthogonal (XZ) projection of the transmigrating monocyte with respect to the endothelial monolayer (dashed line at the position shown in the merged image). Images are representative of at least three independent experiments. (c and d) Polystyrene beads were precoupled with mIgG, anti-PECAM, anti–ICAM-1, or anti–MHC I and were added to HUVECs expressing FLAG-tagged TRPC6. Samples were immunostained with anti-PECAM, anti-FLAG, or anti–VE-cadherin Ab. (e and f) Polystyrene beads precoupled with anti-PECAM were added to TNF-activated HUVECs, which were subsequently fixed and immunostained with one of the following: anti-PECAM, anti-CD99, anti-CD47, or anti–ICAM-1. (c and e) Arrows point to beads. Images are representative of at least three independent experiments. Quantitative analysis of bead experiments represents the mean ± SEM of three independent experiments in which over 800 beads were analyzed per condition. Bars: (a) 50 µm; (b, c, and e) 10 µm. ***, $P < 0.001$ (one- or two-way ANOVA).

↑$[Ca^{2+}]_i$ could rescue TEM by bypassing the PECAM blockade. Interestingly, neutrophils and monocytes that were arrested with anti-PECAM resumed and completed TEM upon endothelial stimulation with OAG (not depicted).

Although OAG is a potent TRPC6 agonist, it is also capable of activating TRPC3 and 7 and protein kinase C (PKC), all of which are naturally activated by DAG. Therefore, to more precisely examine the role of TRPC6 during TEM, we repeated these experiments using Hyp9, a highly selective TRPC6 agonist that has no effect on TRPC3 or 7 at the concentration that we used (Leuner et al., 2010). HUVECs exposed to 10 µM Hyp9 exhibited ↑$[Ca^{2+}]_i$, which could be ablated by monolayer pretreatment with BAPTA-AM (Fig. 4 a). As shown in Fig. 4 c, addition of Hyp9 to HUVECs significantly rescued TEM in the anti-PECAM–blocked neutrophils, whereas addition of vehicle alone did not, similar to results obtained with OAG. Monolayers that were pretreated with BAPTA-AM before Hyp9 treatment did not support TEM (Fig. 4 c), indicating that the ability of Hyp9 to rescue TEM is dependent on endothelial ↑$[Ca^{2+}]_i$ and not caused by off-target effects. Additionally, Hyp9 and OAG had little effect on transendothelial electrical resistance (TEER) compared with

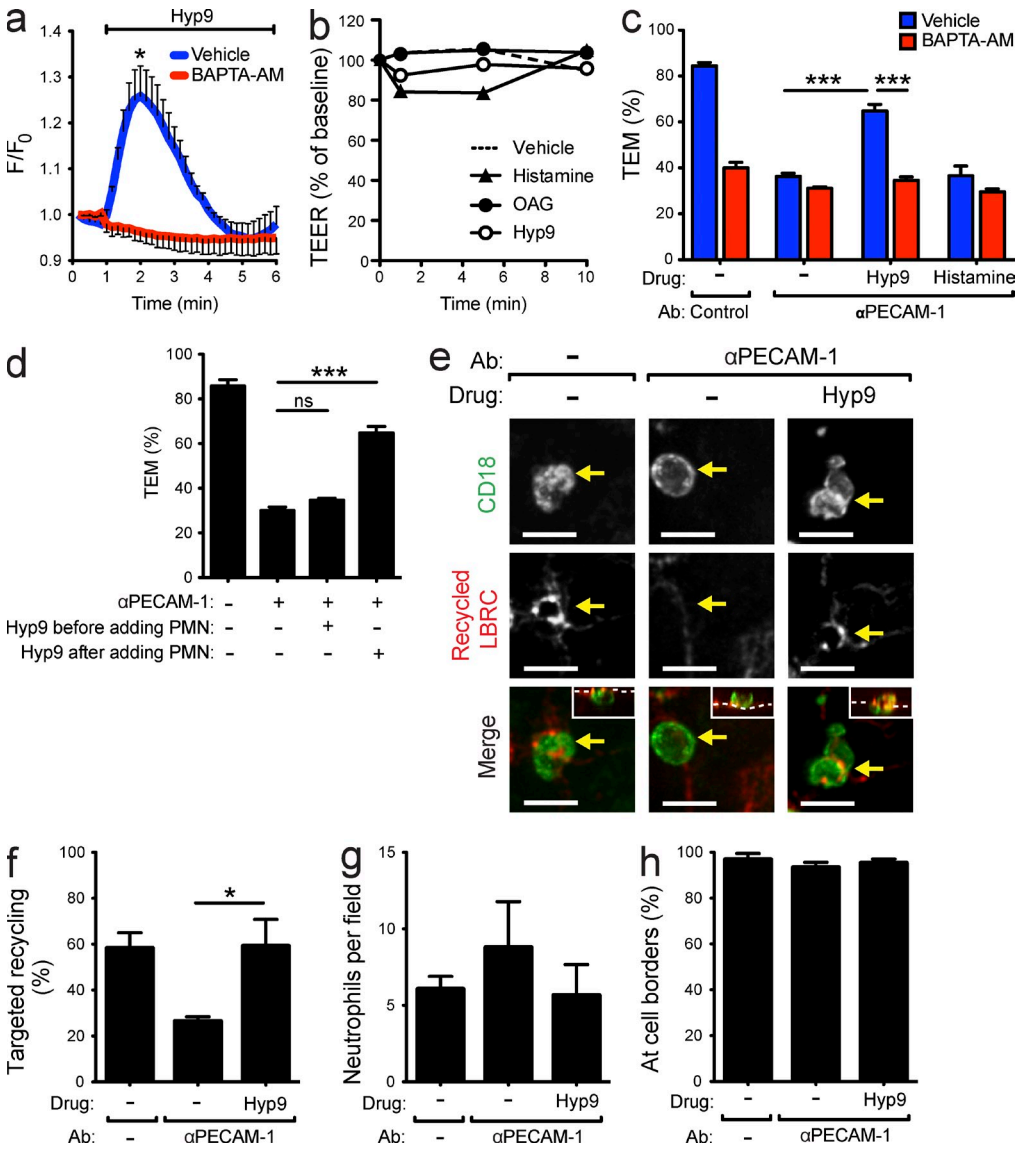

Figure 4. Activation of endothelial TRPC6 is sufficient to rescue TEM and targeted recycling in neutrophils blocked by anti-PECAM Ab. (a) HUVECs were simultaneously loaded with 2.5 µM Fura-2-AM and either 20 µM BAPTA-AM or vehicle (DMSO). Changes in intracellular Ca^{2+} concentration in response to 10 µM Hyp9 were quantified as described in Materials and methods. The plot displays mean ± SEM of the fluorescence/baseline fluorescence (F/F_0) of three independent experiments. At least 60 total cells were individually quantified for each condition. (b) HUVECs seeded on transwell filter plates were treated with vehicle (DMSO), 10 µM histamine (positive control), Hyp9, or OAG for 10 min, and TEER was assessed at various time points. Data are represented as a percentage of baseline TEER (time 0 min). The plot displays mean of three independent experiments in which each condition was tested in triplicate. (c and d) Freshly isolated human neutrophils in the presence of nonblocking anti–VE-cadherin Ab (control) or anti-PECAM Ab were added to HUVECs that were pretreated with 20 µM BAPTA-AM or vehicle. After allowing 10 min for neutrophils to interact with endothelial monolayers, Hyp9, histamine, or vehicle (−) was added to the co-cultures and TEM was allowed to resume for an additional 5 min. Data for c and d were accumulated from the same experiments, and thus, some data in b were redisplayed in c to illustrate the time dependence of Hyp9-mediated rescue of TEM. (e–h) The effect of Hyp9 treatment on LBRC trafficking (e and f), neutrophil adhesion (g), and neutrophil crawling (h) was assessed using our targeted recycling assay, as described in Materials and methods. Arrows denote LBRC enrichment. Cultures in which neutrophils were arrested by anti-PECAM were treated with Hyp9 or vehicle. Insets in e are orthogonal (XZ) projections of arrested or transmigrating neutrophils with respect to the endothelial monolayer (dashed line at the position shown in the merged images). Images are representative of three independent experiments (bars, 10 µm). Quantitative data displayed in c–h represent the mean ± SEM of at least three independent experiments in which each condition was tested in triplicate. *, $P < 0.05$; ***, $P < 0.001$ (two-way ANOVA or Student's *t* test).

vehicle, suggesting their effects on TEM are independent of changes in endothelial barrier function (Fig. 4 b).

In this experiment, both HUVECs and neutrophils were exposed to Hyp9; however, the effect on TEM was abrogated when only endothelial cells were pretreated with BAPTA-AM, demonstrating that endothelial cell Ca^{2+} is required for Hyp9's ability to rescue TEM (Fig. 4 c). These results also suggest that any effects of Hyp9 on the neutrophils had negligible

impact on the experimental outcome. Interestingly, inducing $\uparrow[Ca^{2+}]_i$ with histamine, which mediates acute $\uparrow[Ca^{2+}]_i$ through a store-operated mechanism (Kotlikoff et al., 1987; Riach et al., 1995; Ikeda et al., 1997), did not restore TEM of blocked neutrophils. This suggests that, in contrast to TRPC6-mediated $\uparrow[Ca^{2+}]_i$, a generalized $\uparrow[Ca^{2+}]_i$ is not sufficient to restore TEM in PECAM-blocked neutrophils. Furthermore, the effects of Hyp9 on TEM were dependent on timing, as pretreating HUVECs with Hyp9 before the addition of neutrophils failed to restore TEM in those blocked with anti-PECAM (Fig. 4 d). Together these observations suggest that, in contrast to TRPC6-mediated $\uparrow[Ca^{2+}]_i$, a generalized $\uparrow[Ca^{2+}]_i$ is not sufficient to restore TEM in PECAM-blocked neutrophils and that TRPC6 supports TEM only upon PECAM–PECAM engagement.

To investigate the mechanism by which Hyp9-induced $\uparrow[Ca^{2+}]_i$ rescues TEM in apically arrested neutrophils, we tested the effect of Hyp9 on targeted recycling of the LBRC. Similar to TEM, addition of Hyp9 to co-cultures in which neutrophils were blocked by anti-PECAM fully rescued levels of targeted recycling (Fig. 4, e and f). Hyp9 did not affect neutrophil adhesion or locomotion to the junction (Fig. 4, g and h). Collectively, these data further support our hypothesis that PECAM homophilic interactions are upstream of $\uparrow[Ca^{2+}]_i$ and targeted recycling during TEM and suggest that TRPC6 may be mediating this essential $\uparrow[Ca^{2+}]_i$.

Expression of dominant-negative TRPC6 in endothelial cells attenuates neutrophil TEM and targeted recycling

To more directly test whether TRPC6 channel activity is required for neutrophil TEM, we engineered adenovirus that expresses a FLAG-tagged dominant-negative version of TRPC6 (DN-T6) and transduced HUVEC monolayers for 72 h. This version of TRPC6 contains a mutated pore region through which Ca^{2+} is no longer permeable (Hofmann et al., 1999). HUVECs were loaded with the ratiometric calcium indicator Fura-2 and used to validate the functionality of the DN-T6 protein. Expression of DN-T6 in HUVECs severely blunted $\uparrow[Ca^{2+}]_i$ in response to Hyp9 compared with control monolayers or those expressing a FLAG-tagged WT version of TRPC6 (WT-T6; Fig. 5 a). These data also affirm the specificity of Hyp9, as it barely produced any detectable $\uparrow[Ca^{2+}]_i$ in DN-T6–expressing HUVECs (Fig. 5 a). In response to histamine, which induces $\uparrow[Ca^{2+}]_i$ via a store-operated mechanism (Kotlikoff et al., 1987; Riach et al., 1995; Ikeda et al., 1997), HUVECs expressing DN-T6 exhibited a response similar to those expressing WT-T6 (Fig. 5 a).

In monolayers expressing DN-T6, neutrophil TEM was attenuated by >50% (Fig. 5 c), recapitulating our observations after endothelial Ca^{2+} chelation with BAPTA-AM (Figs. 1 b and 4 b). In stark contrast, monolayers transduced with WT-T6 did not display any aberrant phenotype compared with nontransduced controls (Fig. 5 c). Similarly, HUVEC expression of DN-T6 disrupted targeted recycling by >50%, whereas expression of WT-T6 had no effect (Fig. 5, e and f). Neutrophils were able to adhere and locomote to endothelial borders normally on monolayers expressing DN-T6 (Fig. 5, g and h) but were blocked on the apical surface of the endothelium unable to transmigrate (Fig. 5 e), similar to those observed on BAPTA-AM–treated or anti-PECAM–blocked monolayers. Importantly, the observed attenuation of neutrophil TEM and LBRC targeted recycling in DN-T6–expressing HUVECs cannot be explained by defects in TNF-mediated up-regulation of ICAM-1 (Fig. 5 b). These data indicate that TRPC6 function is critical for neutrophil TEM and trafficking of LBRC membrane.

shRNA knockdown of TRPC6 in endothelial cells attenuates neutrophil TEM but not apical adhesion

As an alternative method of studying the requirement of TRPC6 during TEM, we engineered adenovirus that expressed shRNA specific for TRPC6. The shRNA sequence used to knock down TRPC6 has been shown to have negligible impact on TRPC1, 3, and 4 mRNA levels (Chung et al., 2010).

Transduction of HUVECs with TRPC6 shRNA–expressing adenovirus for 72 h conferred a knockdown of TRPC6 protein of >50% (Fig. 6, a and b). In our quantitative endpoint TEM assay, endothelial TRPC6 knockdown resulted in a significant attenuation of TEM and targeted recycling, similar in extent to DN-T6–expressing monolayers (Fig. 6, c and e). To demonstrate that this phenotype was a result of TRPC6 knockdown, we rescued TRPC6 expression by transducing knockdown HUVECs with adenovirus that expresses TRPC6 transcript in which the targeted nucleotides were mutated to avoid recognition by the shRNA but encode the same amino acid sequence (rescue construct). Re-expression of TRPC6 by the rescue construct in the TRPC6 knockdown cells restored neutrophil TEM and targeted recycling to near-control levels (Fig. 6, c and e). As expected, neutrophil adhesion (Fig. 6, d and f) and neutrophil locomotion to cell borders (Fig. 6 g) were not affected compared with scrambled control.

Chimeric mice deficient in endothelial TRPC6 exhibit a profound defect in leukocyte TEM in a model of acute inflammation

Based on the data we acquired in vitro, we hypothesized that endothelial TRPC6 would be required for efficient neutrophil TEM in vivo during the acute inflammatory response. To distinguish between leukocyte and endothelial TRPC6, we created chimeric mice by reconstituting WT B6 or $TRPC6^{-/-}$ recipients with WT B6 or $TRPC6^{-/-}$ bone marrow. Reconstitution was validated after at least 6 wk via PCR of isolated blood leukocyte genomic DNA (not depicted). We used a model of acute dermatitis of the ear because of its robust inflammatory response and its reproducibility. Equally important, using whole mount preparations of the ear skin, we could examine the precise spatial interactions of leukocytes with endothelium in the ears by confocal microscopy. Croton oil, an inflammatory irritant, was applied to one ear, whereas the diluent was applied to the contralateral ear to serve as an internal negative control. We waited 6–8 h before fixing the tissue, the point at which most neutrophils had

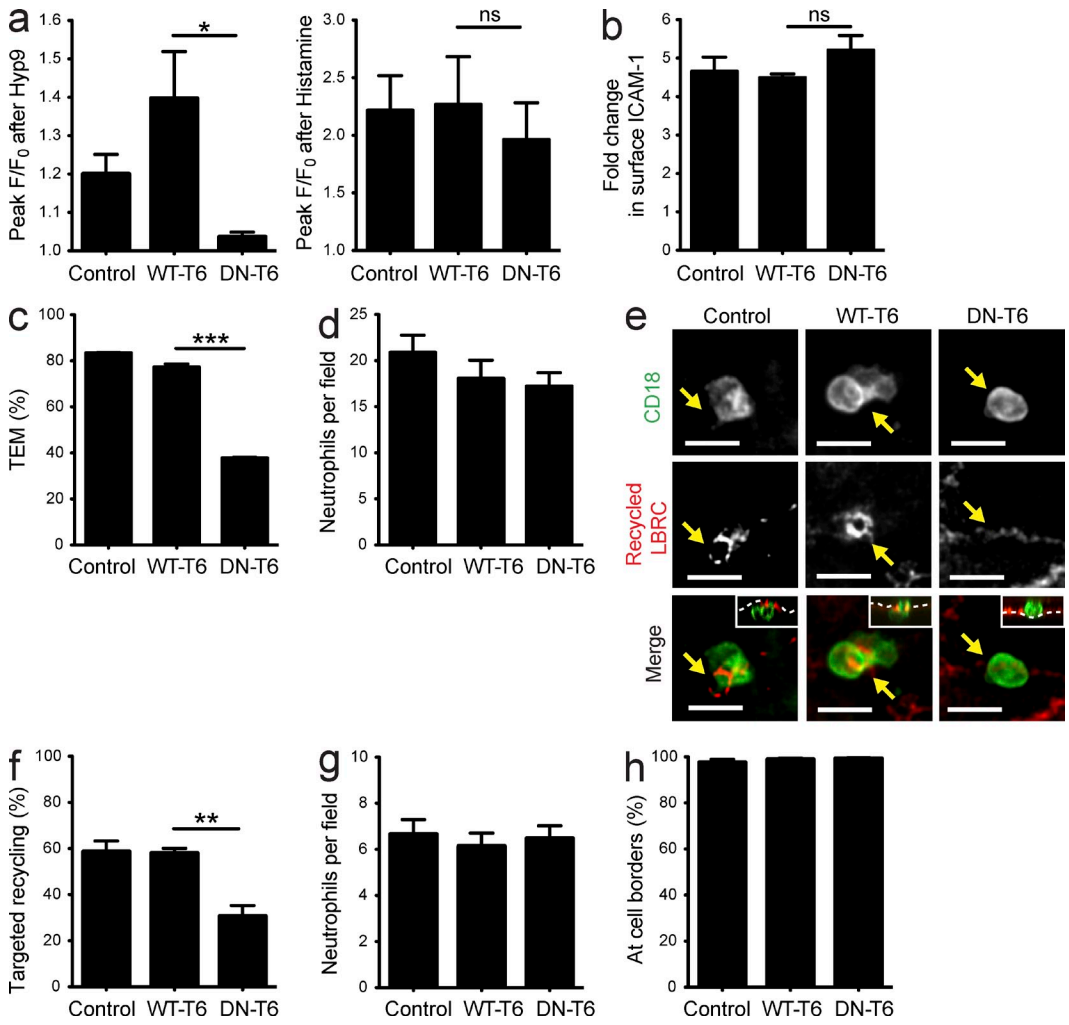

Figure 5. Expression of dominant-negative TRPC6 in endothelial cells attenuates neutrophil TEM and targeted recycling. (a) Nontransduced HUVECs (control) or HUVECs expressing WT FLAG-tagged TRPC6 (WT-T6) or dominant-negative FLAG-tagged TRPC6 (DN-T6) were loaded with 2.5 µM Fura-2-AM. Changes in intracellular Ca^{2+} concentration in response to 10 µM Hyp9 (control $n = 2$, WT-T6 $n = 4$, DN-T6 $n = 4$) or 10 µM histamine (control $n = 3$, WT-T6 $n = 3$, DN-T6 $n = 3$) were quantified as described in Materials and methods. The plots display mean ± SEM of the fluorescence/baseline fluorescence (F/F_0). More than 70 total cells were individually quantified for each condition from three independent experiments. (b) Nontransduced HUVECs (control) or those expressing WT-T6 or DN-T6 were untreated or activated with TNF for 3–4 h and subsequently fixed and immunostained to detect surface ICAM-1. Mean fluorescence intensity of 15 fields was averaged per condition in each experiment. The graph displays mean ± SEM of fold increase in surface ICAM-1 expression in TNF-activated monolayers compared with surface ICAM-1 expression in nonactivated monolayers from three individual experiments. (c and d) Freshly isolated human neutrophils were added to nontransduced HUVECs (control) or those expressing exogenous WT-T6 or DN-T6, and TEM (c) and adhesion (d) were assessed. (e–h) LBRC trafficking (e and f), neutrophil adhesion (g), and neutrophil crawling (h) in WT-T6– and DN-T6–expressing HUVECs were assessed using the targeted recycling assay, as described in Materials and methods. Arrows point to the site where LBRC is or should be enriched (e). Insets in e are orthogonal (XZ) projections of the arrested neutrophil with respect to the endothelial monolayer (dashed line at the position shown in the merged images). Images are representative of three independent experiments (bars, 10 µm). (b–d and f–h) Quantitative data represent the mean ± SEM of at least three independent experiments in which each condition was tested in triplicate. *, $P < 0.05$; **, $P < 0.01$; ***, $P < 0.001$ (one-way ANOVA).

extravasated from the vessel in control animals (Schenkel et al., 2004). The intact tissue was stained for markers of the endothelium, neutrophils, and the basement membrane and then mounted on slides for confocal microscopic analysis. Only postcapillary venules (20–30 µm in diameter), the vasculature through which the majority of leukocyte extravasation occurs (Muller, 2011), were chosen for analysis. Neutrophils were individually assessed in 3D-rendered images based on their position relative to the endothelium and the basement membrane (Fig. 7 b).

Before assessing neutrophil TEM, we sought to ensure that the expression level and distribution of important endothelial adhesion molecules were similar between global $TRPC6^{-/-}$ and WT mice. As shown in Fig. 7 a, there were no noticeable defects in PECAM and ICAM-1 expression patterns in croton oil–treated ears from knockout and WT mice.

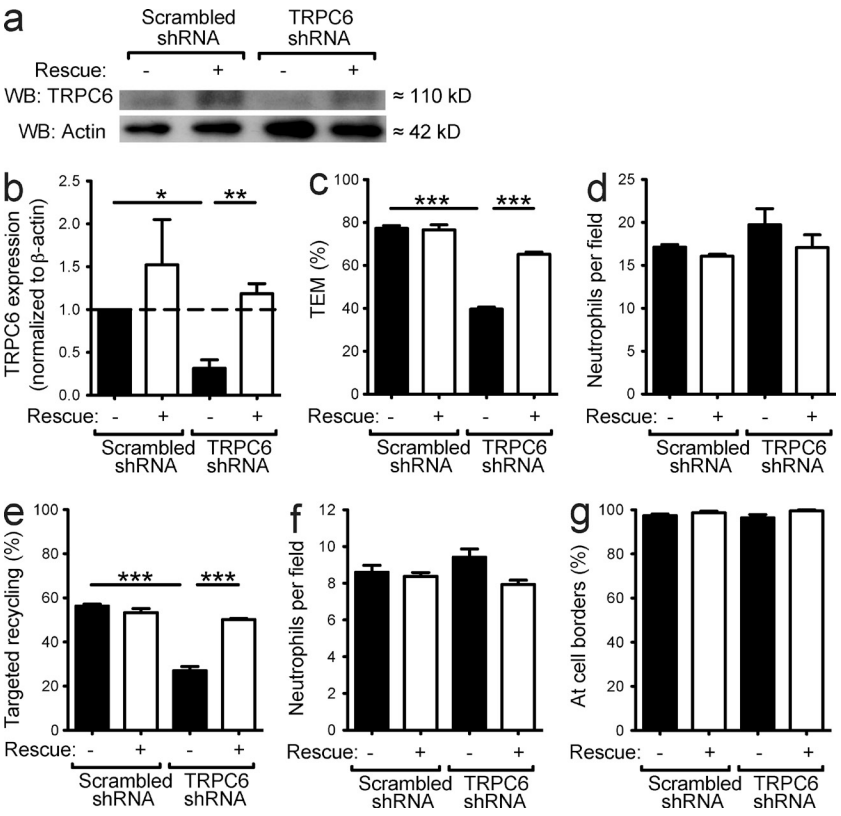

Figure 6. shRNA knockdown of TRPC6 in endothelial cells attenuates neutrophil TEM but not apical adhesion. (a and b) TRPC6 protein levels in HUVECs expressing TRPC6 shRNA or scrambled shRNA, with or without the rescue TRPC6 construct were assessed via Western blot (a). Densitometric analysis was performed and is represented by the mean ± SEM. TRPC6 expression was normalized to β-actin expression from three independent experiments (b). (c–g) Freshly isolated human neutrophils were added to HUVECs expressing TRPC6 shRNA or scrambled shRNA with or without the TRPC6 rescue construct. TEM and adhesion (c and d), as well as targeted recycling, adhesion, and leukocyte crawling (targeted recycling assay, as described in Materials and methods; e–g) were assessed. Quantitative data represent the mean ± SEM of at least three independent experiments in which each condition was tested in triplicate. *, $P < 0.05$; **, $P < 0.01$; ***, $P < 0.001$ (one-way ANOVA).

In mice in which leukocyte extravasation was assessed, the number of neutrophils per 200-µm vessel was nearly identical for all chimeric conditions, indicating that leukocyte trafficking to the inflamed tissue was unaffected by TRPC6 deficiency (Fig. 7 f). In global WT (WT→WT) chimeric mice, ∼80% of all neutrophils transmigrated across the endothelium (Fig. 7, b and e). In contrast, only ∼25% of neutrophils underwent TEM in TRPC6$^{-/-}$ recipients that had received WT bone marrow (Fig. 7, b and e), indicating that endothelial TRPC6 is required for TEM in vivo. The blockade observed in WT→TRPC6$^{-/-}$ chimeric mice was nearly identical to that observed in the global knockout (Fig. 7, b, d, and e). We also observed a significant, but less dramatic defect in TEM in mice where only leukocytes were deficient in TRPC6 (TRPC6$^{-/-}$→WT; not depicted). This was expected, as multiple groups have demonstrated a role for neutrophil and monocyte TRPC6 in chemotaxis (Damann et al., 2009; Lindemann et al., 2013).

When we more closely examined the 3D-rendered confocal images obtained from the WT→TRPC6$^{-/-}$ mice, we noticed that almost all of the neutrophils that had not undergone TEM were still in contact with the luminal surface of the endothelium (Fig. 7 d), similar to the phenotype we observed in vitro when endothelial Ca^{2+} was chelated (Fig. 2 a) or when DN-T6 was expressed (Fig. 5 e). This phenotype is also identical to that observed when PECAM interactions are disrupted both in vitro and in vivo (Muller et al., 1993; Bogen et al., 1994; Schenkel et al., 2004). In these assays, adhesion to the luminal surface requires binding of leukocyte β2 integrins to endothelial ICAM-1 (Liao et al., 1997); therefore, as demonstrated in vitro, adhesion to the endothelium is not affected by loss of endothelial TRPC6. Furthermore, deletion of endothelial TRPC6 does not affect leukocyte transmigration across the basement membrane or chemotaxis, as those neutrophils that were not blocked at the lumen were able to fully extravasate from the vessel (Fig. 7 d). Collectively, these data demonstrate that endothelial TRPC6 is required for neutrophil TEM in vivo but not for neutrophil trafficking to the site of inflammation.

DISCUSSION

A critical role for endothelial ↑$[Ca^{2+}]_i$ during leukocyte TEM has been known for decades (Huang et al., 1993). However, the channels that mediate this critical ↑$[Ca^{2+}]_i$ remained unknown. Here, we report that ↑$[Ca^{2+}]_i$ occurs downstream of leukocyte–endothelial PECAM homophilic interactions and is required for the directed trafficking of LBRC membrane (Figs. 2 and 4). Interestingly, the DAG-activated cation channel TRPC6 colocalizes with PECAM at endothelial cell–cell borders and surrounds leukocytes as they cross the endothelium (Fig. 3). We demonstrate a crucial role for endothelial TRPC6 during neutrophil TEM both in vitro and in vivo, wherein neutrophils maintain their ability to adhere to TRPC6-deficient endothelium and locomote to the cell borders but are unable to transmigrate (Figs. 5, 6, and 7). These data establish TRPC6 as a critical regulator of both TEM and the

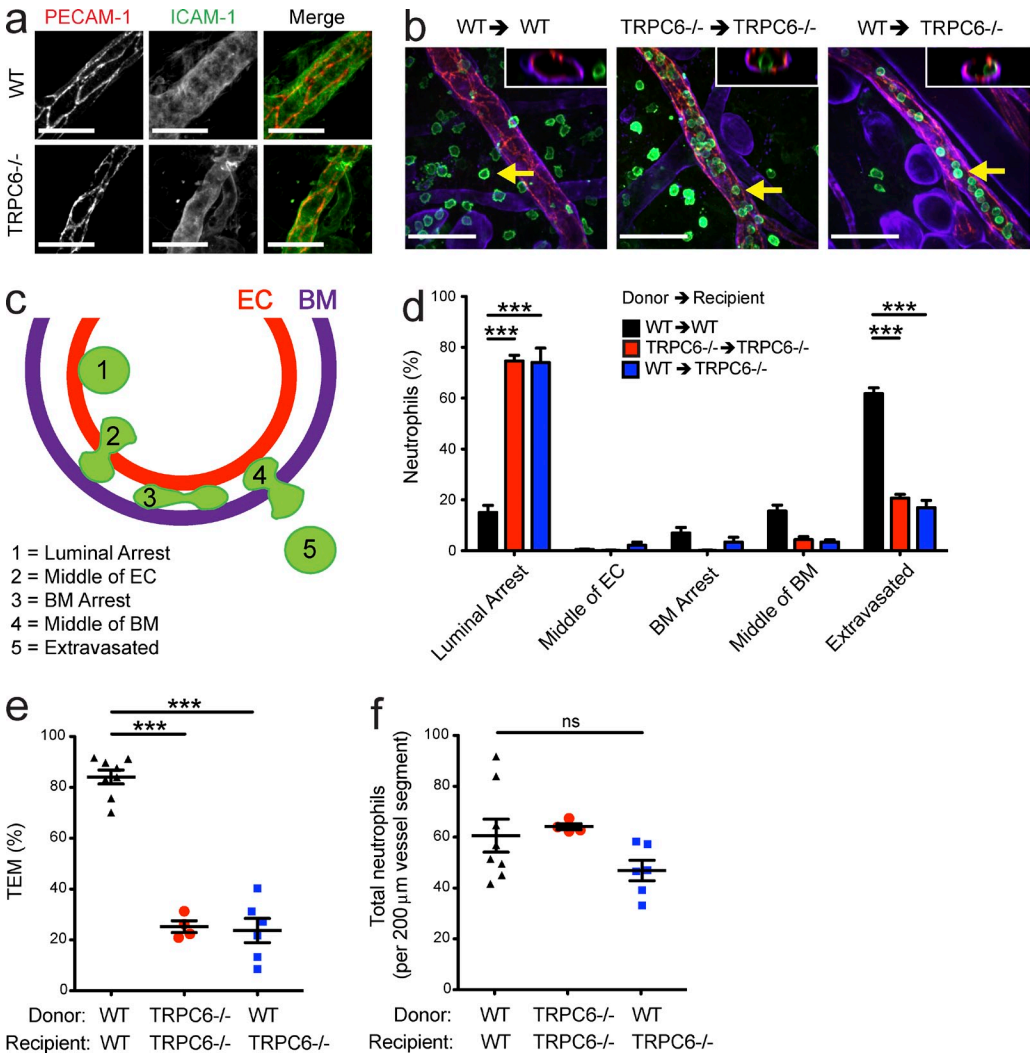

Figure 7. Chimeric mice deficient in endothelial TRPC6 exhibit a profound defect in leukocyte TEM in a model of acute inflammation. (a) WT or TRPC6$^{-/-}$ mice were treated with croton oil on one ear. After 6 h of stimulation, the mice were euthanized and their ears were harvested for immunohistochemical staining with anti-PECAM and anti-ICAM-1. Images are representative of at least 10 fields per mouse (WT $n = 2$ mice, TRPC6$^{-/-}$ $n = 2$ mice). (b–f) WT or TRPC6$^{-/-}$ mice were irradiated and injected with either WT or TRPC6$^{-/-}$ bone marrow. After confirming full reconstitution, they were treated with croton oil on one ear and vehicle on the contralateral ear. After 6 h of stimulation, the mice were euthanized and their ears were harvested for immunohistochemical staining with anti-PECAM (endothelium, red), anti-collagen IV (basement membrane, purple), and anti-MRP14 (neutrophils, green). (b) Representative images of the ears. Insets display an orthogonal view to illustrate the site of neutrophil arrest. Arrows denote the predominating site of neutrophil position relative to the endothelium. (a and b) Bars, 50 µm. (c) Diagram outlining the scoring of neutrophil position relative to the endothelium and basement membrane. (d) Quantification of neutrophil position. (e) Quantification of the percentage neutrophil TEM. (f) Quantification of the number of neutrophils per 200 µm of vessel (i.e., neutrophil trafficking to the site of inflammation). Over 100 neutrophils were scored per mouse (WT→WT $n = 8$ mice, TRPC6$^{-/-}$→TRPC6$^{-/-}$ $n = 4$ mice, WT→TRPC6$^{-/-}$ $n = 6$ mice) in each of two independent experiments. Quantitative data in d–f are represented as the mean ± SEM. ***, $P < 0.001$ (one- or two-way ANOVA).

inflammatory response and illuminate a novel pathway that governs TEM.

Previous investigations have shown that Ab-mediated cross-linking of P- or E-selectin or vascular cell adhesion molecule-1 (VCAM-1), but not ICAM-1, on activated HUVECs produced a detectable transient increase in cytosolic free calcium ion concentration. Unlike TRPC6-mediated Ca^{2+} influx, these signals were mediated by Ca^{2+} store release from the endoplasmic reticulum, and their relationship to TEM was not investigated (Lorenzon et al., 1998; Cook-Mills et al., 2004; Peterson et al., 2005). Our study demonstrates that the ↑$[Ca^{2+}]_i$ required for TEM is distinct from calcium signals that may be initiated by ligation of endothelial cell adhesion molecules other than PECAM. In many of our experiments, neutrophils and monocytes were free to interact with ICAM-1 and VCAM-1 on cytokine-activated endothelial cells. Yet, when PECAM interactions were blocked, TEM was severely attenuated (Figs. 1 and 4). Thus, any ↑$[Ca^{2+}]_i$

initiated by ICAM-1 or VCAM-1 was not sufficient to promote TEM when leukocyte–endothelial PECAM interactions were disrupted. Only TRPC6 activation by the DAG analogue OAG or TRPC6-selective agonist Hyp9, which were only effective when given after leukocytes were arrested by anti-PECAM but not before (Fig. 4 d), was capable of rescuing TEM and targeted recycling of the LBRC (Fig. 4, c and f). Furthermore, in contrast to beads coated with anti-PECAM, those coated with anti–ICAM-1 failed to recruit TRPC6 (Fig. 3, c and d).

Before our study, endothelial TRPC6 function during leukocyte–endothelial cell interactions and its signaling relationship to PECAM had not been investigated. However, several groups have illustrated other functions of TRPC6 during the inflammatory response (Hofmann et al., 1999; Singh et al., 2007; Sel et al., 2008; Damann et al., 2009; Hamid and Newman, 2009; Kini et al., 2010; Tauseef et al., 2012; Thilo et al., 2012b; Weissmann et al., 2012; Lindemann et al., 2013; Wu et al., 2015). For example, endothelial TRPC6 mediates increases in endothelial permeability in response to various soluble inflammatory mediators (Leung et al., 2006; Singh et al., 2007; Kini et al., 2010; Tauseef et al., 2012). These findings provided a strong incentive to study TRPC6 in detail in the context of leukocyte–endothelial interactions.

Many of the previously published studies cited above describe defects in the inflammatory response in TRPC6$^{-/-}$ mice (Sel et al., 2008; Davis et al., 2012; Tauseef et al., 2012; Weissmann et al., 2012; Lindemann et al., 2013). However, none of these authors investigated leukocyte TEM as the step at which inflammation might be inhibited. Given our new findings, one could extrapolate ways in which the defects observed in TRPC6$^{-/-}$ mice in past studies may have been affected by decreased leukocyte TEM. In Lindemann et al. (2013) and Tauseef et al. (2012), the investigators observed that TRPC6$^{-/-}$ mice were significantly protected from thioglycollate-induced peritonitis and LPS-induced lung inflammation, respectively. Although the authors attributed these observations to defects in neutrophil chemotaxis and TLR-4 signaling, it is likely that their observed phenotypes were at least partially influenced by attenuation in leukocyte TEM. TRPC6$^{-/-}$ mice also display defective wound healing (Davis et al., 2012). The authors attribute this phenotype to disrupted myofibroblast differentiation; however, their data do not exclude the possibility of a defect in monocyte extravasation, which is also critical for proper wound healing.

It is important to note that endothelial permeability and leukocyte TEM are distinct processes, even though many of their signaling pathways intersect at various points. For example, cortactin deficiency in mice leads to increased vascular permeability but attenuated neutrophil extravasation (Schnoor et al., 2011). Also, VE-cadherin contains two tyrosine phosphorylation sites that differentially regulate endothelial permeability and adherens junction reorganization during TEM (Wessel et al., 2014). These findings demonstrate that merely destabilizing endothelial junctions is not sufficient to permit leukocyte TEM or vice versa. Consistent with this assessment, application of the TRPC6-selective agonist Hyp9 rescues TEM in the face of an ongoing anti-PECAM blockade without affecting endothelial barrier function (Fig. 4, b and c). Extrapolating from this, we postulate that endothelial TRPC6 function in permeability is independent from its function in TEM.

Cross-linking of PECAM Ig domain 6 (the heterophilic interaction domain, which has no role in TEM) was shown to induce a sustained Ca^{2+} influx mediated by an unidentified nonspecific cation channel that is independent of voltage-gated and store-operated Ca^{2+} channels (Gurubhagavatula et al., 1998; O'Brien et al., 2001). The characteristics of this sustained Ca^{2+} flux are considerably different in both kinetics and amplitude from the transient $\uparrow[Ca^{2+}]_i$ mediated by TRPC6 in response to Hyp9 or OAG (Leuner et al., 2010; Tauseef et al., 2012).

Over a decade ago, Su et al. (2000) published data showing that endothelial cells adjacent to a transmigration event undergo a single, global $\uparrow[Ca^{2+}]_i$. We used various Ca^{2+}-sensitive dyes, biosensors, and imaging techniques to reproduce this data, but we were ultimately unable to do so. In most of the hundreds of TEM events we recorded live, we failed to observe any reproducible global increases in endothelial $\uparrow[Ca^{2+}]_i$ during neutrophil TEM. Neither can we induce a global $\uparrow[Ca^{2+}]_i$ by cross-linking PECAM using mAbs against extracellular Ig domains 1 and 2 (unpublished data). We believe that the endothelial $\uparrow[Ca^{2+}]_i$ during TEM involves subtle, localized signals at the site of transmigration rather than one global $\uparrow[Ca^{2+}]_i$.

In corroboration with this assessment, we show that TRPC6 at the cell–cell border surrounds leukocytes that are in the process of transmigrating (Fig. 3 b). Junctional proteins that facilitate TEM, like PECAM and CD99, also display this pattern, suggesting that the junctional fraction of endothelial TRPC6 may promote leukocyte TEM. Although we were unable to coimmunoprecipitate PECAM with TRPC6 (not depicted), a functional relationship between the two proteins clearly exists, as anti-PECAM–coated beads recruit TRPC6 exclusively rather than as a component of a protein complex of surface molecules that regulate TEM (Fig. 3, c, e, and f). TRPC6 that is recruited to anti-PECAM beads may come from the junctional plasma membrane or, alternatively, from internal stores that are shuttled to the surface, which has been reported by other groups (Cayouette et al., 2004; Fleming et al., 2007; Chaudhuri et al., 2008; Keserü et al., 2008; Xie et al., 2012). We plan to address this question in future studies in hopes of yielding new insight into the mechanism by which PECAM signaling regulates and/or augments TRPC6-mediated $\uparrow[Ca^{2+}]_i$.

Collectively, these observations highlight a spatially selective role for TRPC6, wherein the channel may mediate $\uparrow[Ca^{2+}]_i$ in the area surrounding the transmigration event. This would make sense biologically as well. Localized calcium signaling is a hallmark of cytoskeletal rearrangement in other biological contexts, such as the immunological synapse and the leading edge of migrating cells (Kummerow et al.,

2009; Wei et al., 2009; Schwindling et al., 2010). In contrast, processes involving cell proliferation of transcription factor activation typically require global changes in cytosolic calcium concentration (Feske et al., 2001; Schwarz et al., 2007). TRPC6 has also been shown to reside in lipid raft microdomains at the plasma membrane wherein intracellular signaling, including Ca^{2+} influx, is spatially restricted (Lei et al., 2014). Lastly, TRPC6 is known to be more tightly regulated and has a lower channel conductance than other TRPC isoforms, like TRPC3 (Zitt et al., 1997; Hofmann et al., 1999; Zhang et al., 2001; Kim et al., 2012). Therefore, one would expect TRPC6 to function in a restricted, spatiotemporal manner during TEM. However, the $\uparrow[Ca^{2+}]_i$ induced by the TRPC6-selective agonist Hyp9 when supplied in solution is global (quantified in Figs. 4 A and 6 A). This may not accurately represent how TRPC6 functions during TEM, as pharmacologic experiments tend to lack the nuance that is exhibited under physiological conditions. This observed global signal may also be a result of sustained opening of the channel caused by a surplus of drug in solution.

Because the LBRC traffics to the site of TEM (Mamdouh et al., 2003) and TRPC6 is required for this trafficking (Figs. 5 f and 6 e), the junctional fraction of TRPC6 may provide a small, but localized $\uparrow[Ca^{2+}]_i$ to mediate targeted recycling. Our experiments provide evidence for this, as $\uparrow[Ca^{2+}]_i$ occurs upstream of targeted recycling and junctional opening (Fig. 2). Also, endothelial Ca^{2+} chelation and disruption of TRPC6 function arrests leukocytes on the apical surface of the endothelium rather than in the middle or on the basolateral side (Figs. 2, 4, 5, and 6), indicating that TRPC6-mediated $\uparrow[Ca^{2+}]_i$ occurs at an early stage in the process. This is in contrast to the $\uparrow[Ca^{2+}]_i$ that may be required for barrier restoration or pore closure during the latter stages of leukocyte TEM, as postulated by Martinelli et al. (2013).

Beyond LBRC trafficking, other Ca^{2+}-dependent mechanisms are known to regulate TEM. Myosin light chain kinase (MLCK), which is activated by Ca^{2+}/calmodulin, mediates phosphorylation of myosin light chain II to induce endothelial cell contraction. Pharmacological inhibition of its function attenuates neutrophil TEM (Garcia et al., 1998; Saito et al., 1998). Interestingly, TRPC6-mediated $\uparrow[Ca^{2+}]_i$ regulates endothelial permeability in response to LPS and thrombin by activating MLCK to induce cytoskeletal rearrangement (Singh et al., 2007; Tauseef et al., 2012). Furthermore, MLCK has been shown to induce β-catenin dissociation from VE-cadherin in brain endothelial cells (Beard et al., 2014), a process that is critical for TEM. Thus, a similar pathway involving TRPC6 and MLCK may govern other cellular events required for TEM.

There are many ways in which PECAM homophilic interactions may be activating TRPC6. PECAM has been described as an important sensor of shear or mechanical stress, subsequently signaling to an associated G protein–coupled receptor (GPCR) or receptor tyrosine kinase (RTK) at the plasma membrane (Tzima et al., 2005; Yeh et al., 2008; Otte et al., 2009; dela Paz et al., 2014). Activation of GPCR or RTK by PECAM sensing results in activation of one of the PLC isoforms, which catalyzes the reaction to produce local DAG. In the context of TEM, this signaling mechanism could explain how PECAM homophilic interactions or mechanical stress from the leukocyte engaging endothelial cell PECAM triggers local DAG increases and subsequent TRPC6-mediated $\uparrow[Ca^{2+}]_i$. Alternatively, TRPC6 has been reported to be directly activated by membrane stretch (Spassova et al., 2006; Anderson et al., 2013). Once the leukocyte has initiated TEM through PECAM-dependent interactions, leukocyte pressure on the endothelial junction may directly activate TRPC6. Experiments addressing the mechanism by which PECAM signals to TRPC6, though beyond the scope of this study, are underway and should provide novel insight into PECAM-mediated intracellular signaling.

In summary, we have identified that the increase in cytosolic Ca^{2+} in endothelial cells required for TEM occurs downstream of PECAM–PECAM interactions and is mediated by TRPC6. Our findings highlight a novel function for TRPC6 during TEM and the inflammatory response. Leukocyte–endothelial PECAM interactions lead to TRPC6 activation, which then mediates LBRC trafficking to surround the leukocyte and promote subsequent migration across the endothelium. TRPC6-selective pharmacological inhibitors, especially if targeted to the endothelium, could be used as an effective antiinflammatory therapy. Future studies will focus on mechanisms governing PECAM signaling to TRPC6, how TRPC6-mediated $\uparrow[Ca^{2+}]_i$ regulates trafficking of the LBRC, and its potential role in cytoskeletal/junctional reorganization during TEM.

MATERIALS AND METHODS

All procedures involving human subjects and human materials were approved by the Institutional Review Board at Northwestern University Feinberg School of Medicine.

Animals. All procedures were approved by the Institutional Animal Care and Use Committee of Northwestern University and University of Illinois. C57BL/6J WT mice and *Trpc6*$^{-/-}$ mice on a C57BL/6J background were raised and housed at both Northwestern University Feinberg School of Medicine and University of Illinois in Chicago.

Abs and reagents. Mouse IgG2a anti–human PECAM (clone Hec7), mouse IgG2a anti–human VE-cadherin (clone hec1), mouse IgG2a anti–human CD18 (clone IB4), Armenian hamster anti–mouse PECAM (clone 2H8), mouse IgG2a anti–human ICAM-1 (clone R6.5), and mouse IgG2a anti–human MHC I (clone W6/32) were produced in the laboratory using hybridoma Ab production and purification (Muller et al., 1989; Ali et al., 1997). Rabbit polyclonal anti–human PECAM (#177) was raised against the extracellular portion of human PECAM. Rabbit anti–human β-actin, rabbit anti–mouse collagen IV, and rat anti–mouse MRP-14 were purchased from Abcam. Nonspecific mouse IgG1, goat anti–mouse IgG, goat anti–rabbit IgG, and goat anti–Armenian hamster IgG were purchased from Jackson ImmunoResearch Laboratories, Inc. DyLight-488, -550, and -650 goat anti–mouse IgG2a and DyLight-550 goat anti–Armenian hamster were conjugated using a kit purchased from Thermo Fisher Scientific. Mouse IgG1 anti–human TRPC6 (clone 3F2.H10.F2), nonconjugated and Cy3-conjugated mouse IgG1 anti-FLAG (clone M2), histamine dihydrochloride, Hyp9, OAG, BAPTA-AM, and probenecid were purchased from Sigma-Aldrich. Fura-2 and Fluo-4 calcium indicators were purchased from Life Technologies.

Isolation and culture of endothelial cells. HUVECs were isolated from human umbilical cords as previously described (Muller et al., 1989, 1993). After two passages, HUVECs were cultured on 3D type I collagen matrices (PureCol; Inamed Biomaterials) to mimic physiological basement membranes (Muller et al., 1989; Muller and Luscinskas, 2008). For adenoviral infection, HUVECs were infected for 72 h with shRNA and TRPC6-expressing adenoviruses.

Isolation of human PBMCs and neutrophils. PBMCs were isolated as previously described (Muller and Weigl, 1992; Muller and Luscinskas, 2008). In brief, blood was drawn from healthy volunteers into 1/10 volume EDTA (10 mM) and mixed with an equal volume of HBSS (Corning). Blood/HBSS mixture was layered over Ficoll-Paque density gradient medium (GE Healthcare) and centrifuged at 2,200 rpm for 20 min. The upper plasma layer was collected. The PBMC layer was collected and diluted in HBSS. Both PBMCs and plasma were centrifuged at 1,500 rpm for 10 min. The PBMC pellet was resuspended in the spun platelet-depleted plasma and centrifuged at 1,200 rpm for 5 min. The resulting PBMC pellet was washed three times with HBSS via resuspension and centrifugation at 1,200 rpm for 5 min. The final PBMC pellet was resuspended in M199 (Life Technologies) containing 0.1% human serum albumin (HSA; Grifols Biological Inc.).

For isolation of human neutrophils, blood was drawn from healthy volunteers into 1/10 volume EDTA (10 mM). Blood was layered over Polymorphprep (Cosmo Bio USA Inc.) and centrifuged at 1,800 rpm for 30 min. The middle layer was collected and diluted in HBSS. Three total washes were performed via resuspension and centrifugation at 750 rpm for 5 min. The final pellet was resuspended in M199 containing 0.1% HSA.

Cloning of shRNA and TRPC6 adenoviral constructs. TRPC6 shRNA (5′-GCGACAGAGCATCATTGACGCAAATCTGTGAAGCCACAGATGGGATTTGCGTCAATGATGCTCTGGTGCTTTTTT-3′) and scrambled control (5′-GCGCGTAGTAATGACAATCCGCGCTCTGTGAAGCCACAGATGGGAGCGCGGATTGTCATTACTACTTGCTTTTTT-3′) were provided in the pAd-track vector by B. Sanborn, Y.-S. Kim, and A.E. Ulloa (Colorado State University, Fort Collins, CO). The shRNA constructs and hU6 promoters were cloned into the pENTR4 plasmid (Life Technologies). These vectors were recombined with the adenoviral vector pAd/PL-DEST (Life Technologies) using LR clonase (Life Technologies) according to the manufacturer's guidelines and used to produce adenovirus for transduction according to standard methods (Zhang et al., 2006).

The full-length, N-terminally FLAG-tagged WT TRPC6 (WT-T6) and dominant-negative TRPC6 (DN-T6) constructs were provided by J. Schlöndorff (Beth Israel Deaconess Medical Center, Boston, MA; Schlöndorff et al., 2009). DN-T6 was originally generated by PCR mutagenesis whereby the conserved LFW amino acid sequence (Δ678–680) was changed to AAA from full-length TRPC6 cDNA (Hofmann et al., 2002). The LFW motif enables Ca^{2+} permeabilization through the putative pore region of TRPC6. WT-T6 and DN-T6 sequences were subsequently cloned into the pENTR4 vector with a pCMV promoter. To generate TRPC6-mCherry, non-FLAG–tagged WT-T6 was inserted in frame with mCherry in the pENTRY4 vector, encoding C-terminal mCherry–linked fusion protein. Site-directed mutagenesis was performed on WT-T6 to generate the rescue TRPC6 construct. Six silent point mutations were introduced such that the TRPC6 shRNA would no longer recognize a portion of TRPC6 mRNA. All construct sequences were validated via sequencing analysis at the Northwestern University Center for Genetic Medicine.

For adenoviral transduction, HUVECs were seeded on 3D collagen matrices (96 well), fibronectin-coated MatTek dishes or fibronectin- and collagen-coated Ibidi flow chambers. The next day, monolayers were washed three times with serum-free M199 and incubated with adenovirus for up to 24 h. Adenoviral media was subsequently replaced with fresh culture media until the day of the experiment. For all experiments, shRNA and TRPC6 constructs were expressed for ∼72 h.

Polystyrene microsphere (bead) coating and recruitment experiments. Polystyrene microspheres were coated as previously described (Sullivan et al., 2013). In brief, amino-functionalized 3-mm polystyrene beads (Polysciences) were washed and resuspended in 8% glutaraldehyde in PBS for 2 h at room temperature. Beads were then washed and incubated with 200 µg/ml anti-PECAM mAb, anti–ICAM-1 mAb, anti–MHC I mAb, or control mIgG1 for 2 h at room temperature. Lastly, beads were incubated with 0.1 M glycine in PBS for 2 h at room temperature and stored in PBS for up to 48 h before use. For bead recruitment experiments, HUVEC monolayers were grown on fibronectin-coated MatTek dishes and transduced for 72 h with FLAG-tagged WT-T6. The day of the experiment, beads were washed and diluted in preconditioned HUVEC media before being added back to the dishes. Beads were allowed to settle and bind for 20 min at 37°C. Samples were subsequently fixed with 4% paraformaldehyde, permeabilized, and stained with fluorescently labeled anti-PECAM, anti–VE-cadherin, and anti-FLAG Abs (Fig. 3, c and d) or labeled with anti-PECAM, anti-CD47, anti-CD99, or anti–ICAM-1, followed by addition of a fluorescently conjugated secondary Ab (Fig. 3, e and f).

Immunofluorescence microscopy. Confluent HUVECs were washed with PBS and fixed in 4% paraformaldehyde for 10 min at 37°C. Cells were then washed three times and permeabilized with 0.01% Triton X-100 for 10 min at room temperature. Blocking buffer (PBS + 2.5% BSA, 2.5% FBS, and 2.5% host species serum) was added for 1 h at room temperature. Cells were then incubated with fluorescently labeled primary Ab at 20 µg/ml in blocking buffer for 1 h at room temperature. Confocal images were visualized using an UltraVIEW VoX imaging system (PerkinElmer) equipped with a CSU-1 spinning disk (Yokogawa Electric Corporation). Images were acquired with a 40× oil immersion objective using Volocity software (PerkinElmer). All images were processed and analyzed with ImageJ software (National Institutes of Health).

Western blotting. HUVECs were washed twice with cold PBS (with Ca^{2+} and Mg^{2+}) and subsequently lysed in a buffer containing cold PBS (without Ca^{2+} and Mg^{2+}), 1% NP-40, and one tablet of complete Mini protease inhibitor cocktail (Roche). Lysates were then added to an equal volume of 2× Laemmli buffer and heated at 60°C for 30 min. Total cell lysates were separated by 8% SDS-PAGE and transferred to PVDF (Sigma-Aldrich). Standard Western blotting techniques were then performed to detect desired protein levels.

TEM assay. TEM assays were performed as previously described (Muller et al., 1993; Lou et al., 2007; Muller and Luscinskas, 2008). For experiments in which monocyte TEM was evaluated, freshly isolated PBMCs were added to resting HUVEC monolayers. Alternatively, neutrophil TEM assays required HUVEC activation with 20 ng/ml human recombinant TNF (R&D Systems) for at least 3 h. Preactivation of HUVECs with cytokine before this assay did not affect the rate of monocyte TEM, adhesion, or the efficacy of Ab blockade. PECAM and CD99 were constitutively expressed at endothelial borders. Thus, treatment with proinflammatory cytokines TNF or IL-1β did not alter their expression levels or distribution (Schenkel et al., 2002).

In brief, 100 µl PBMC suspension (2×10^6 cells/ml) was added to each well of confluent HUVEC monolayers grown on hydrated type I collagen gels and allowed to migrate for 1 h at 37°C in 5% CO_2. Monolayers were washed twice with 1 mM EDTA in PBS (no Ca^{2+} and Mg^{2+}) and then twice with PBS (with Ca^{2+} and Mg^{2+}) before being fixed in 1% glutaraldehyde in 0.1 M sodium cacodylate buffer (Electron Microscopy Sciences). Fixed cells were stained with modified Wright-Giemsa stain (Protocol Hema3; Thermo Fisher Scientific) and mounted on glass slides.

Similarly, 100 µl neutrophils (0.25×10^6 cells/ml) were added to TNF-activated HUVECs and allowed to migrate for 15 min. Monolayers were washed twice with PBS (with Ca^{2+} and Mg^{2+}) and fixed, stained, and mounted as described above.

For each sample, at least 100 leukocytes per monolayer were scored using an Ultraphot microscope (Carl Zeiss) with Nomarski optics and a SPOT Insight Color CCD (Diagnostic Instruments Inc.). Leukocytes were scored based on their position relative to the endothelial nuclei: above or below.

For TEM assays in which PECAM homophilic interactions were blocked, anti-PECAM was added to the leukocyte suspension for 5 min before their addition to HUVEC monolayers. Excess Ab in the leukocyte suspension was included upon addition to the HUVEC monolayers.

For TEM assays in which $\uparrow[Ca^{2+}]_i$ was inhibited by BAPTA-AM, HUVECs were preincubated with either vehicle (DMSO) or 20 µM BAPTA-AM in culture-conditioned media at 37°C for 40 min. 2.5 mM probenecid (Sigma-Aldrich), a cation efflux transporter inhibitor, was also included in the media to prevent BAPTA leakage. HUVECs were then washed extensively in warm M199 before addition of leukocytes.

For TEM assays in which endothelial cells expressed shRNA or TRPC6 adenoviral constructs, HUVECs were transduced for ∼72 h (as described above). For TEM assays in which neutrophils were rescued by addition of the selective TRPC6 agonist Hyp9 (Sigma-Aldrich), neutrophils were blocked with anti-PECAM as described above and subsequently added to HUVEC monolayers for 10 min. At this time point, vehicle (DMSO), 10 µM Hyp9, or 10 µM histamine (Sigma-Aldrich) was added to the HUVEC/neutrophil co-cultures, and TEM was allowed to resume for an additional 5 min before fixation.

Targeted recycling assay. Targeted recycling assays were performed as previously described (Mamdouh et al., 2003, 2008, 2009). In brief, HUVEC monolayers were grown to confluency on hydrated type 1 collagen matrix. HUVECs were incubated with nonblocking PECAM Fab IgG2a (clone P1.1) in HUVEC-conditioned media for 1 h at 37°C. In some experiments a functional blocking rabbit anti-PECAM IgG (20 µg/ml) was added to some wells. Monolayers were subsequently washed, chilled, and incubated with a saturating amount (100 µg/ml) of nonconjugated goat anti–mouse IgG2a (Jackson ImmunoResearch Laboratories, Inc.) for 1 h at 4°C to bind surface anti-PECAM mAb. After extensive washing of unbound Ab, PBMCs (2×10^6 cells/ml) or PMNs (0.25×10^6) were added to monolayers along with DyLight-550 goat anti–mouse IgG2a in M199. Monolayer were kept at 4°C for 15 min to allow leukocytes to settle before being warmed to 37°C for 10 min (for PBMCs) or 5 min (for neutrophils) at 5% CO_2. Cells were subsequently washed and fixed in 4% paraformaldehyde for 10 min at 4°C. Fixed samples were stained with Alexa Fluor 488 anti-CD18 (clone IB4) and imaged using 3D confocal microscopy. Confocal images were visualized as described in Immunofluorescence microscopy.

For each sample, at least five fields and 20 total cells per monolayer were counted and scored according to their position relative to endothelial junctions, whether or not they had initiated TEM (as determined by orthogonal view) and whether or not there was appreciable enrichment PECAM-bearing membrane (at least 1.5-fold higher fluorescence than junctional PECAM) around the migrating cells (targeted recycling). For experiments in which Hyp9 was used to rescue targeted recycling during anti-PECAM blockade, 10 µM Hyp9 was added to monolayers after the neutrophils had settled and, thus, immediately before continuation of the assay at 37°C. This method ensured that the drug's effect on $\uparrow[Ca^{2+}]_i$ would occur at the precise time at which neutrophils were initiating TEM/targeted recycling.

Bone marrow transplantation. WT and *Trpc6*$^{-/-}$ mice were irradiated with 1,000 rads (10 Gy). Approximately 24 h after irradiation, mice were injected retroorbitally with 0.2 ml of 3×10^6 donor bone marrow cells (*Trpc6*$^{-/-}$ or WT) using a 27-gauge needle. Experiments were performed at least 6 wk after bone marrow transfer. Complete bone marrow constitution of the chimeric mice was confirmed using PCR analysis.

Croton oil–induced dermatitis. Croton oil experiments were performed as previously described (Schenkel et al., 2004). In brief, both male and female age- and sex-matched chimeric mice were exposed to 2% croton oil (Sigma-Aldrich) in a 4:1 mixture of acetone/olive oil (diluent) on one ear. The contralateral ear was treated with vehicle solution alone. After 6 h the animals were sacrificed. The ears were harvested and fixed in 4% paraformaldehyde overnight at 4°C. Tissue was permeabilized and blocked in a solution of 0.3% Triton X-100, 2.5% BSA, and 2.5% host species serum in PBS for 24 h at 4°C. Ears were then incubated with anti-PECAM (clone 2H8), anti–ICAM-1 (clone YN1/1.7.4; Abcam), anti–MRP-14 (Abcam), or anti–collagen IV (Abcam) in blocking solution overnight at 4°C. Tissue was then incubated with secondary Ab (Dylight550 goat anti–Armenian hamster, Alexa Fluor 488 goat anti–rat, or Alexa Fluor 647 goat anti–rabbit at 1:500) in PBS for 4 h at room temperature.

Stained tissue was mounted on glass slides, and postcapillary venules of 20–30 µm were imaged using an UltraVIEW VoX imaging system equipped with a CSU-1 spinning disk. Images were analyzed using Volocity software, which renders the optical sections into 3D images, thus allowing one to discern the position of leukocytes relative of the endothelium and basement membrane.

Cytosolic Ca^{2+} measurements. Ibidi flow chambers of 0.4-µm thickness were coated with poly-L-lysine for 5 min. Chambers were then coated with 250 µg/ml type 1 collagen in H_2O for 1.5 h, followed by a coating with 50 µg/ml fibronectin for 15 min. HUVECs were then plated on the bottom of the chambers and used at least 3 d after plating.

Fura-2-AM (Sigma-Aldrich) was reconstituted in a 20% Pluronic acid + DMSO solution (Life Technologies) and then diluted in M199 + 2.5 mM probenecid to a final concentration of 2.5 µM (loading buffer). HUVECs were incubated with Fura-2 loading buffer for 50 min at 37°C. If BAPTA-AM was used in the experiment, it was simultaneously loaded with Fura-2-AM at a final concentration of 20 µM.

HUVECs were equilibrated for at least 10 min at 1.5 dyne/cm^2 shear flow using M199 without phenol red. After a brief baseline recording, 10 µM Hyp9 or 10 µM histamine was introduced into the chamber, and images were recorded for an additional 6 min.

Images were acquired using MetaFluor software (Molecular Devices) on a DMI 6000B microscope (Leica) equipped with a C10600 camera and 40× oil objective (Hamamatsu Photonics). 340-nm/380-nm ratios were determined in ImageJ (National Institutes of Health) by outlining each individual cell in the field and measuring changes in 340-nm/380-nm ratio. Final figures represent the 340-nm/380-nm value at any given frame over the baseline measurement of the first frame (F/F_0).

TEER. Endothelial barrier function was tested as previously described (Winger et al., 2014). In brief, HUVECs were seeded on 3-mm transwell filter inserts (Corning) that were precoated with collagen type I (1:50 dilution) in 60% ethanol followed by a coating of 5 mg/ml fibronectin. For each filter, the electrical resistance was measured using an electrical resistance system containing a current passing and voltage-measuring electrode (World Precision Instruments). The mean resistance of three blank filters was subtracted from filters in which HUVECs were plated to account for background TEER. Resistance calculations were normalized to filter surface area before being represented as a percentage of baseline TEER (time 0 min).

Statistical analysis. Numerical values represent the mean of at least three independent experiments ± SEM. Variance of mean values between two groups was analyzed by the Student's *t* test for unpaired observations. Group differences were tested with one-way ANOVA (or two-way ANOVA when appropriate) followed by the Bonferroni's multiple comparison post-hoc test to calculate p-values. *, $P < 0.05$; **, $P < 0.01$; ***, $P < 0.001$. Statistical analyses were performed using Prism software (GraphPad Software).

We would like to acknowledge Dr. Cliff Carpenter for his assistance with cell culture experiments, Dr. David Sullivan for valuable training and mentorship, and all members of the Muller laboratory for their insightful feedback and thoughtful discussion. We are grateful to Dr. Barbara M. Sanborn, Dr. Yoon-Sun Kim, and Dr. Aida E. Ulloa for generously providing the shRNA constructs and Johannes Schlöndorff for generously providing the FLAG-TRPC6 constructs. We wish to thank Larry Wong and Praveen Thumbikat for sharing their Fura-2 microscope setup and acknowledge the DNA Sequencing Core facility for excellent service.

This work was supported by the National Institutes of Health (NIH; grants R01HL046849 and R37HL064774 to W.A. Muller) and predoctoral training grants

from the American Heart Association (14PRE18550021 and 12PRE9330014 to E.W. Weber) and in part by the Intramural Research Division of the NIH (grant ZO1-ES-101684 to L. Birnbaumer). Publication of this research was supported by the Sidney & Bess Eisenberg Memorial Fund.

The authors declare no competing financial interests.

Submitted: 26 February 2015
Accepted: 25 August 2015

REFERENCES

Ali, J., F. Liao, E. Martens, and W.A. Muller. 1997. Vascular endothelial cadherin (VE-cadherin): cloning and role in endothelial cell-cell adhesion. *Microcirculation*. 4:267–277. http://dx.doi.org/10.3109/10739689709146790

Allport, J.R., W.A. Muller, and F.W. Luscinskas. 2000. Monocytes induce reversible focal changes in vascular endothelial cadherin complex during transendothelial migration under flow. *J. Cell Biol.* 148:203–216. http://dx.doi.org/10.1083/jcb.148.1.203

Anderson, M., E.Y. Kim, H. Hagmann, T. Benzing, and S.E. Dryer. 2013. Opposing effects of podocin on the gating of podocyte TRPC6 channels evoked by membrane stretch or diacylglycerol. *Am. J. Physiol. Cell Physiol.* 305:C276–C289. http://dx.doi.org/10.1152/ajpcell.00095.2013

Beard, R.S. Jr., R.J. Haines, K.Y. Wu, J.J. Reynolds, S.M. Davis, J.E. Elliott, N.L. Malinin, V. Chatterjee, B.J. Cha, M.H. Wu, and S.Y. Yuan. 2014. Non-muscle Mlck is required for β-catenin- and FoxO1-dependent downregulation of Cldn5 in IL-1β-mediated barrier dysfunction in brain endothelial cells. *J. Cell Sci.* 127:1840–1853. http://dx.doi.org/10.1242/jcs.144550

Berman, M.E., Y. Xie, and W.A. Muller. 1996. Roles of platelet/endothelial cell adhesion molecule-1 (PECAM-1, CD31) in natural killer cell transendothelial migration and beta 2 integrin activation. *J. Immunol.* 156:1515–1524.

Bogen, S., J. Pak, M. Garifallou, X. Deng, and W.A. Muller. 1994. Monoclonal antibody to murine PECAM-1 (CD31) blocks acute inflammation in vivo. *J. Exp. Med.* 179:1059–1064. http://dx.doi.org/10.1084/jem.179.3.1059

Carman, C.V., and T.A. Springer. 2004. A transmigratory cup in leukocyte diapedesis both through individual vascular endothelial cells and between them. *J. Cell Biol.* 167:377–388. http://dx.doi.org/10.1083/jcb.200404129

Cayouette, S., M.P. Lussier, E.L. Mathieu, S.M. Bousquet, and G. Boulay. 2004. Exocytotic insertion of TRPC6 channel into the plasma membrane upon G_q protein-coupled receptor activation. *J. Biol. Chem.* 279:7241–7246. http://dx.doi.org/10.1074/jbc.M312042200

Chaudhuri, P., S.M. Colles, M. Bhat, D.R. Van Wagoner, L. Birnbaumer, and L.M. Graham. 2008. Elucidation of a TRPC6-TRPC5 channel cascade that restricts endothelial cell movement. *Mol. Biol. Cell.* 19:3203–3211. http://dx.doi.org/10.1091/mbc.E07-08-0765

Chung, D., Y.S. Kim, J.N. Phillips, A. Ulloa, C.Y. Ku, H.L. Galan, and B.M. Sanborn. 2010. Attenuation of canonical transient receptor potential-like channel 6 expression specifically reduces the diacylglycerol-mediated increase in intracellular calcium in human myometrial cells. *Endocrinology*. 151:406–416. http://dx.doi.org/10.1210/en.2009-0085

Cook-Mills, J.M., J.D. Johnson, T.L. Deem, A. Ochi, L. Wang, and Y. Zheng. 2004. Calcium mobilization and Rac1 activation are required for VCAM-1 (vascular cell adhesion molecule-1) stimulation of NADPH oxidase activity. *Biochem. J.* 378:539–547. http://dx.doi.org/10.1042/bj20030794

Damann, N., G. Owsianik, S. Li, C. Poll, and B. Nilius. 2009. The calcium-conducting ion channel transient receptor potential canonical 6 is involved in macrophage inflammatory protein-2-induced migration of mouse neutrophils. *Acta Physiol. (Oxf.)*. 195:3–11. http://dx.doi.org/10.1111/j.1748-1716.2008.01918.x

Dasgupta, B., E. Dufour, Z. Mamdouh, and W.A. Muller. 2009. A novel and critical role for tyrosine 663 in platelet endothelial cell adhesion molecule-1 trafficking and transendothelial migration. *J. Immunol.* 182:5041–5051. http://dx.doi.org/10.4049/jimmunol.0803192

Dasgupta, B., T. Chew, A. deRoche, and W.A. Muller. 2010. Blocking platelet/endothelial cell adhesion molecule 1 (PECAM) inhibits disease progression and prevents joint erosion in established collagen antibody-induced arthritis. *Exp. Mol. Pathol.* 88:210–215. http://dx.doi.org/10.1016/j.yexmp.2009.09.013

Davis, J., A.R. Burr, G.F. Davis, L. Birnbaumer, and J.D. Molkentin. 2012. A TRPC6-dependent pathway for myofibroblast transdifferentiation and wound healing in vivo. *Dev. Cell.* 23:705–715. http://dx.doi.org/10.1016/j.devcel.2012.08.017

dela Paz, N.G., B. Melchior, F.Y. Shayo, and J.A. Frangos. 2014. Heparan sulfates mediate the interaction between platelet endothelial cell adhesion molecule-1 (PECAM-1) and the $G\alpha_{q/11}$ subunits of heterotrimeric G proteins. *J. Biol. Chem.* 289:7413–7424. http://dx.doi.org/10.1074/jbc.M113.542514

Dietrich, A., and T. Gudermann. 2007. TRPC6. *Handbook Exp. Pharmacol.* 179:125–141. http://dx.doi.org/10.1007/978-3-540-34891-7_7

Dietrich, A., M. Mederos y Schnitzler, J. Emmel, H. Kalwa, T. Hofmann, and T. Gudermann. 2003. N-linked protein glycosylation is a major determinant for basal TRPC3 and TRPC6 channel activity. *J. Biol. Chem.* 278:47842–47852. http://dx.doi.org/10.1074/jbc.M302983200

Etienne-Manneville, S., J.B. Manneville, P. Adamson, B. Wilbourn, J. Greenwood, and P.O. Couraud. 2000. ICAM-1-coupled cytoskeletal rearrangements and transendothelial lymphocyte migration involve intracellular calcium signaling in brain endothelial cell lines. *J. Immunol.* 165:3375–3383. http://dx.doi.org/10.4049/jimmunol.165.6.3375

Feske, S., J. Giltnane, R. Dolmetsch, L.M. Staudt, and A. Rao. 2001. Gene regulation mediated by calcium signals in T lymphocytes. *Nat. Immunol.* 2:316–324. http://dx.doi.org/10.1038/86318

Fleming, I., A. Rueben, R. Popp, B. Fisslthaler, S. Schrodt, A. Sander, J. Haendeler, J.R. Falck, C. Morisseau, B.D. Hammock, and R. Busse. 2007. Epoxyeicosatrienoic acids regulate Trp channel–dependent Ca^{2+} signaling and hyperpolarization in endothelial cells. *Arterioscler. Thromb. Vasc. Biol.* 27:2612–2618. http://dx.doi.org/10.1161/ATVBAHA.107.152074

Garcia, J.G., A.D. Verin, M. Herenyiova, and D. English. 1998. Adherent neutrophils activate endothelial myosin light chain kinase: role in transendothelial migration. *J. Appl. Physiol.* 84:1817–1821.

Gurubhagavatula, I., Y. Amrani, D. Pratico, F.L. Ruberg, S.M. Albelda, and R.A. Panettieri Jr. 1998. Engagement of human PECAM-1 (CD31) on human endothelial cells increases intracellular calcium ion concentration and stimulates prostacyclin release. *J. Clin. Invest.* 101:212–222. http://dx.doi.org/10.1172/JCI269

Hamid, R., and J.H. Newman. 2009. Evidence for inflammatory signaling in idiopathic pulmonary artery hypertension: TRPC6 and nuclear factor-κB. *Circulation*. 119:2297–2298. http://dx.doi.org/10.1161/CIRCULATIONAHA.109.855197

Hofmann, T., A.G. Obukhov, M. Schaefer, C. Harteneck, T. Gudermann, and G. Schultz. 1999. Direct activation of human TRPC6 and TRPC3 channels by diacylglycerol. *Nature*. 397:259–263. http://dx.doi.org/10.1038/16711

Hofmann, T., M. Schaefer, G. Schultz, and T. Gudermann. 2002. Subunit composition of mammalian transient receptor potential channels in living cells. *Proc. Natl. Acad. Sci. USA*. 99:7461–7466. http://dx.doi.org/10.1073/pnas.102596199

Horinouchi, T., T. Higa, H. Aoyagi, T. Nishiya, K. Terada, and S. Miwa. 2012. Adenylate cyclase/cAMP/protein kinase A signaling pathway inhibits endothelin type A receptor-operated Ca^{2+} entry mediated via transient receptor potential canonical 6 channels. *J. Pharmacol. Exp. Ther.* 340:143–151. http://dx.doi.org/10.1124/jpet.111.187500

Huang, A.J., J.E. Manning, T.M. Bandak, M.C. Ratau, K.R. Hanser, and S.C. Silverstein. 1993. Endothelial cell cytosolic free calcium regulates neutrophil migration across monolayers of endothelial cells. *J. Cell Biol.* 120:1371–1380. http://dx.doi.org/10.1083/jcb.120.6.1371

Ikeda, H., N. Kubo, A. Nakamura, N. Harada, M. Minamino, and T. Yamashita. 1997. Histamine-induced calcium released from cultured human mucosal microvascular endothelial cells from nasal inferior turbinate. *Acta Otolaryngol.* 117:864–870. http://dx.doi.org/10.3109/00016489709114216

Keserü, B., E. Barbosa-Sicard, R. Popp, B. Fisslthaler, A. Dietrich, T. Gudermann, B.D. Hammock, J.R. Falck, N. Weissmann, R. Busse, and I. Fleming. 2008. Epoxyeicosatrienoic acids and the soluble epoxide

hydrolase are determinants of pulmonary artery pressure and the acute hypoxic pulmonary vasoconstrictor response. *FASEB J.* 22:4306–4315. http://dx.doi.org/10.1096/fj.08-112821

Kielbassa-Schnepp, K., A. Strey, A. Janning, L. Missiaen, B. Nilius, and V. Gerke. 2001. Endothelial intracellular Ca^{2+} release following monocyte adhesion is required for the transendothelial migration of monocytes. *Cell Calcium.* 30:29–40. http://dx.doi.org/10.1054/ceca.2001.0210

Kim, Y., A.C. Wong, J.M. Power, S.F. Tadros, M. Klugmann, A.J. Moorhouse, P.P. Bertrand, and G.D. Housley. 2012. Alternative splicing of the TRPC3 ion channel calmodulin/IP3 receptor-binding domain in the hindbrain enhances cation flux. *J. Neurosci.* 32:11414–11423. http://dx.doi.org/10.1523/JNEUROSCI.6446-11.2012

Kini, V., A. Chavez, and D. Mehta. 2010. A new role for PTEN in regulating transient receptor potential canonical channel 6-mediated Ca^{2+} entry, endothelial permeability, and angiogenesis. *J. Biol. Chem.* 285:33082–33091. http://dx.doi.org/10.1074/jbc.M110.142034

Kotlikoff, M.I., R.K. Murray, and E.E. Reynolds. 1987. Histamine-induced calcium release and phorbol antagonism in cultured airway smooth muscle cells. *Am. J. Physiol.* 253:C561–C566.

Kummerow, C., C. Junker, K. Kruse, H. Rieger, A. Quintana, and M. Hoth. 2009. The immunological synapse controls local and global calcium signals in T lymphocytes. *Immunol. Rev.* 231:132–147. http://dx.doi.org/10.1111/j.1600-065X.2009.00811.x

Lei, L., S. Lu, Y. Wang, T. Kim, D. Mehta, and Y. Wang. 2014. The role of mechanical tension on lipid raft dependent PDGF-induced TRPC6 activation. *Biomaterials.* 35:2868–2877. http://dx.doi.org/10.1016/j.biomaterials.2013.12.030

Leuner, K., J.H. Heiser, S. Derksen, M.I. Mladenov, C.J. Fehske, R. Schubert, M. Gollasch, G. Schneider, C. Harteneck, S.S. Chatterjee, and W.E. Müller. 2010. Simple 2,4-diacylphloroglucinols as classic transient receptor potential-6 activators—identification of a novel pharmacophore. *Mol. Pharmacol.* 77:368–377. http://dx.doi.org/10.1124/mol.109.057513

Leung, P.C., K.T. Cheng, C. Liu, W.T. Cheung, H.Y. Kwan, K.L. Lau, Y. Huang, and X. Yao. 2006. Mechanism of non-capacitative Ca^{2+} influx in response to bradykinin in vascular endothelial cells. *J. Vasc. Res.* 43:367–376. http://dx.doi.org/10.1159/000094096

Ley, K., C. Laudanna, M.I. Cybulsky, and S. Nourshargh. 2007. Getting to the site of inflammation: the leukocyte adhesion cascade updated. *Nat. Rev. Immunol.* 7:678–689. http://dx.doi.org/10.1038/nri2156

Liao, F., J. Ali, T. Greene, and W.A. Muller. 1997. Soluble domain 1 of platelet-endothelial cell adhesion molecule (PECAM) is sufficient to block transendothelial migration in vitro and in vivo. *J. Exp. Med.* 185:1349–1358. http://dx.doi.org/10.1084/jem.185.7.1349

Lindemann, O., D. Umlauf, S. Frank, S. Schimmelpfennig, J. Bertrand, T. Pap, P.J. Hanley, A. Fabian, A. Dietrich, and A. Schwab. 2013. TRPC6 regulates CXCR2-mediated chemotaxis of murine neutrophils. *J. Immunol.* 190:5496–5505. http://dx.doi.org/10.4049/jimmunol.1201502

Liu, Y., F. Echtermeyer, F. Thilo, G. Theilmeier, A. Schmidt, R. Schülein, B.L. Jensen, C. Loddenkemper, V. Jankowski, N. Marcussen, et al. 2012. The proteoglycan syndecan 4 regulates transient receptor potential canonical 6 channels via RhoA/Rho-associated protein kinase signaling. *Arterioscler. Thromb. Vasc. Biol.* 32:378–385. http://dx.doi.org/10.1161/ATVBAHA.111.241018

Lorenzon, P., E. Vecile, E. Nardon, E. Ferrero, J.M. Harlan, F. Tedesco, and A. Dobrina. 1998. Endothelial cell E- and P-selectin and vascular cell adhesion molecule-1 function as signaling receptors. *J. Cell Biol.* 142:1381–1391. http://dx.doi.org/10.1083/jcb.142.5.1381

Lou, O., P. Alcaide, F.W. Luscinskas, and W.A. Muller. 2007. CD99 is a key mediator of the transendothelial migration of neutrophils. *J. Immunol.* 178:1136–1143. http://dx.doi.org/10.4049/jimmunol.178.2.1136

Mamdouh, Z., X. Chen, L.M. Pierini, F.R. Maxfield, and W.A. Muller. 2003. Targeted recycling of PECAM from endothelial surface-connected compartments during diapedesis. *Nature.* 421:748–753. http://dx.doi.org/10.1038/nature01300

Mamdouh, Z., G.E. Kreitzer, and W.A. Muller. 2008. Leukocyte transmigration requires kinesin-mediated microtubule-dependent membrane trafficking from the lateral border recycling compartment. *J. Exp. Med.* 205:951–966. http://dx.doi.org/10.1084/jem.20072328

Mamdouh, Z., A. Mikhailov, and W.A. Muller. 2009. Transcellular migration of leukocytes is mediated by the endothelial lateral border recycling compartment. *J. Exp. Med.* 206:2795–2808. http://dx.doi.org/10.1084/jem.20082745

Martinelli, R., M. Kamei, P.T. Sage, R. Massol, L. Varghese, T. Sciuto, M. Toporsian, A.M. Dvorak, T. Kirchhausen, T.A. Springer, and C.V. Carman. 2013. Release of cellular tension signals self-restorative ventral lamellipodia to heal barrier micro-wounds. *J. Cell Biol.* 201:449–465. http://dx.doi.org/10.1083/jcb.201209077

Möller, C.C., C. Wei, M.M. Altintas, J. Li, A. Greka, T. Ohse, J.W. Pippin, M.P. Rastaldi, S. Wawersik, S. Schiavi, et al. 2007. Induction of TRPC6 channel in acquired forms of proteinuric kidney disease. *J. Am. Soc. Nephrol.* 18:29–36. http://dx.doi.org/10.1681/ASN.2006091010

Muller, W.A. 1992. PECAM-1: an adhesion molecule at the junctions of endothelial cells. In Mononuclear Phagocytes: Biology of Monocytes and Macrophages. R. van Furth, editor. Springer Netherlands, Dordrecht. pp. 138–148.

Muller, W.A. 2011. Mechanisms of leukocyte transendothelial migration. *Annu. Rev. Pathol.* 6:323–344. http://dx.doi.org/10.1146/annurev-pathol-011110-130224

Muller, W.A., and F.W. Luscinskas. 2008. Assays of transendothelial migration in vitro. *Methods Enzymol.* 443:155–176. http://dx.doi.org/10.1016/S0076-6879(08)02009-0

Muller, W.A., and S.A. Weigl. 1992. Monocyte-selective transendothelial migration: dissection of the binding and transmigration phases by an in vitro assay. *J. Exp. Med.* 176:819–828. http://dx.doi.org/10.1084/jem.176.3.819

Muller, W.A., C.M. Ratti, S.L. McDonnell, and Z.A. Cohn. 1989. A human endothelial cell-restricted, externally disposed plasmalemmal protein enriched in intercellular junctions. *J. Exp. Med.* 170:399–414. http://dx.doi.org/10.1084/jem.170.2.399

Muller, W.A., S.A. Weigl, X. Deng, and D.M. Phillips. 1993. PECAM-1 is required for transendothelial migration of leukocytes. *J. Exp. Med.* 178:449–460. http://dx.doi.org/10.1084/jem.178.2.449

O'Brien, C.D., G. Ji, Y.X. Wang, J. Sun, V.P. Krymskaya, F.L. Ruberg, M.I. Kotlikoff, and S.M. Albelda. 2001. PECAM-1 (CD31) engagement activates a phosphoinositide-independent, nonspecific cation channel in endothelial cells. *FASEB J.* 15:1257–1260. http://dx.doi.org/10.1083/jcb.200110056

Otte, L.A., K.S. Bell, L. Loufrani, J.C. Yeh, B. Melchior, D.N. Dao, H.Y. Stevens, C.R. White, and J.A. Frangos. 2009. Rapid changes in shear stress induce dissociation of a $G\alpha_{q/11}$–platelet endothelial cell adhesion molecule-1 complex. *J. Physiol.* 587:2365–2373. http://dx.doi.org/10.1113/jphysiol.2009.172643

Paria, B.C., S.M. Vogel, G.U. Ahmmed, S. Alamgir, J. Shroff, A.B. Malik, and C. Tiruppathi. 2004. Tumor necrosis factor-α-induced TRPC1 expression amplifies store-operated Ca^{2+} influx and endothelial permeability. *Am. J. Physiol. Lung Cell. Mol. Physiol.* 287:L1303–L1313. http://dx.doi.org/10.1152/ajplung.00240.2004

Peterson, M.D., E. Vlasova, C. Di Ciano-Oliveira, G.P. Downey, M.I. Cybulsky, A. Kapus, and T.K. Waddell. 2005. Monocyte-induced endothelial calcium signaling mediates early xenogeneic endothelial activation. *Am. J. Transplant.* 5:237–247. http://dx.doi.org/10.1111/j.1600-6143.2004.00666.x

Reiser, J., K.R. Polu, C.C. Möller, P. Kenlan, M.M. Altintas, C. Wei, C. Faul, S. Herbert, I. Villegas, C. Avila-Casado, et al. 2005. TRPC6 is a glomerular slit diaphragm-associated channel required for normal renal function. *Nat. Genet.* 37:739–744. http://dx.doi.org/10.1038/ng1592

Riach, R.A., G. Duncan, M.R. Williams, and S.F. Webb. 1995. Histamine and ATP mobilize calcium by activation of H1 and P2u receptors in human lens epithelial cells. *J. Physiol.* 486:273–282. http://dx.doi.org/10.1113/jphysiol.1995.sp020810

Saito, H., Y. Minamiya, M. Kitamura, S. Saito, K. Enomoto, K. Terada, and J. Ogawa. 1998. Endothelial myosin light chain kinase regulates neutrophil migration across human umbilical vein endothelial cell monolayer. *J. Immunol.* 161:1533–1540.

Schenkel, A.R., Z. Mamdouh, X. Chen, R.M. Liebman, and W.A. Muller. 2002. CD99 plays a major role in the migration of monocytes through endothelial junctions. *Nat. Immunol.* 3:143–150. http://dx.doi.org/10.1038/ni749

Schenkel, A.R., T.W. Chew, and W.A. Muller. 2004. Platelet endothelial cell adhesion molecule deficiency or blockade significantly reduces leukocyte emigration in a majority of mouse strains. *J. Immunol.* 173:6403–6408. http://dx.doi.org/10.4049/jimmunol.173.10.6403

Schlöndorff, J., D. Del Camino, R. Carrasquillo, V. Lacey, and M.R. Pollak. 2009. TRPC6 mutations associated with focal segmental glomerulosclerosis cause constitutive activation of NFAT-dependent transcription. *Am. J. Physiol. Cell Physiol.* 296:C558–C569. http://dx.doi.org/10.1152/ajpcell.00077.2008

Schnoor, M., F.P. Lai, A. Zarbock, R. Kläver, C. Polaschegg, D. Schulte, H.A. Weich, J.M. Oelkers, K. Rottner, and D. Vestweber. 2011. Cortactin deficiency is associated with reduced neutrophil recruitment but increased vascular permeability in vivo. *J. Exp. Med.* 208:1721–1735. http://dx.doi.org/10.1084/jem.20101920

Schwarz, E.C., C. Kummerow, A.S. Wenning, K. Wagner, A. Sappok, K. Waggershauser, D. Griesemer, B. Strauss, M.J. Wolfs, A. Quintana, and M. Hoth. 2007. Calcium dependence of T cell proliferation following focal stimulation. *Eur. J. Immunol.* 37:2723–2733. http://dx.doi.org/10.1002/eji.200737039

Schwindling, C., A. Quintana, E. Krause, and M. Hoth. 2010. Mitochondria positioning controls local calcium influx in T cells. *J. Immunol.* 184:184–190. http://dx.doi.org/10.4049/jimmunol.0902872

Sel, S., B.R. Rost, A.O. Yildirim, B. Sel, H. Kalwa, H. Fehrenbach, H. Renz, T. Gudermann, and A. Dietrich. 2008. Loss of classical transient receptor potential 6 channel reduces allergic airway response. *Clin. Exp. Allergy.* 38:1548–1558. http://dx.doi.org/10.1111/j.1365-2222.2008.03043.x

Shaw, S.K., P.S. Bamba, B.N. Perkins, and F.W. Luscinskas. 2001. Real-time imaging of vascular endothelial-cadherin during leukocyte transmigration across endothelium. *J. Immunol.* 167:2323–2330. http://dx.doi.org/10.4049/jimmunol.167.4.2323

Shi, J., E. Mori, Y. Mori, M. Mori, J. Li, Y. Ito, and R. Inoue. 2004. Multiple regulation by calcium of murine homologues of transient receptor potential proteins TRPC6 and TRPC7 expressed in HEK293 cells. *J. Physiol.* 561:415–432. http://dx.doi.org/10.1113/jphysiol.2004.075051

Singh, I., N. Knezevic, G.U. Ahmmed, V. Kini, A.B. Malik, and D. Mehta. 2007. $G\alpha_q$-TRPC6-mediated Ca^{2+} entry induces RhoA activation and resultant endothelial cell shape change in response to thrombin. *J. Biol. Chem.* 282:7833–7843. http://dx.doi.org/10.1074/jbc.M608288200

Spassova, M.A., T. Hewavitharana, W. Xu, J. Soboloff, and D.L. Gill. 2006. A common mechanism underlies stretch activation and receptor activation of TRPC6 channels. *Proc. Natl. Acad. Sci. USA.* 103:16586–16591. http://dx.doi.org/10.1073/pnas.0606894103

Su, W.H., H.I. Chen, J.P. Huang, and C.J. Jen. 2000. Endothelial $[Ca^{2+}]_i$ signaling during transmigration of polymorphonuclear leukocytes. *Blood.* 96:3816–3822.

Su, W.-H., H.I. Chen, and C.J. Jen. 2002. Differential movements of VE-cadherin and PECAM-1 during transmigration of polymorphonuclear leukocytes through human umbilical vein endothelium. *Blood.* 100:3597–3603. http://dx.doi.org/10.1182/blood-2002-01-0303

Sullivan, D.P., M.A. Seidman, and W.A. Muller. 2013. Poliovirus receptor (CD155) regulates a step in transendothelial migration between PECAM and CD99. *Am. J. Pathol.* 182:1031–1042. http://dx.doi.org/10.1016/j.ajpath.2012.11.037

Sullivan, D.P., C. Rüffer, and W.A. Muller. 2014. Isolation of the lateral border recycling compartment using a diaminobenzidine-induced density shift. *Traffic.* 15:1016–1029. http://dx.doi.org/10.1111/tra.12184

Tauseef, M., N. Knezevic, K.R. Chava, M. Smith, S. Sukriti, N. Gianaris, A.G. Obukhov, S.M. Vogel, D.E. Schraufnagel, A. Dietrich, et al. 2012. TLR4 activation of TRPC6-dependent calcium signaling mediates endotoxin-induced lung vascular permeability and inflammation. *J. Exp. Med.* 209:1953–1968. http://dx.doi.org/10.1084/jem.20111355

Thilo, F., Y. Liu, C. Loddenkemper, R. Schuelein, A. Schmidt, Z. Yan, Z. Zhu, A. Zakrzewicz, M. Gollasch, and M. Tepel. 2012a. VEGF regulates TRPC6 channels in podocytes. *Nephrol. Dial. Transplant.* 27:921–929. http://dx.doi.org/10.1093/ndt/gfr457

Thilo, F., B.J. Vorderwülbecke, A. Marki, K. Krueger, Y. Liu, D. Baumunk, A. Zakrzewicz, and M. Tepel. 2012b. Pulsatile atheroprone shear stress affects the expression of transient receptor potential channels in human endothelial cells. *Hypertension.* 59:1232–1240. http://dx.doi.org/10.1161/HYPERTENSIONAHA.111.183608

Tzima, E., M. Irani-Tehrani, W.B. Kiosses, E. Dejana, D.A. Schultz, B. Engelhardt, G. Cao, H. DeLisser, and M.A. Schwartz. 2005. A mechanosensory complex that mediates the endothelial cell response to fluid shear stress. *Nature.* 437:426–431. http://dx.doi.org/10.1038/nature03952

Wei, C., X. Wang, M. Chen, K. Ouyang, L.S. Song, and H. Cheng. 2009. Calcium flickers steer cell migration. *Nature.* 457:901–905. http://dx.doi.org/10.1038/nature07577

Weissmann, N., A. Sydykov, H. Kalwa, U. Storch, B. Fuchs, M. Mederos y Schnitzler, R.P. Brandes, F. Grimminger, M. Meissner, M. Freichel, et al. 2012. Activation of TRPC6 channels is essential for lung ischaemia–reperfusion induced oedema in mice. *Nat. Commun.* 3:649. http://dx.doi.org/10.1038/ncomms1660

Wessel, F., M. Winderlich, M. Holm, M. Frye, R. Rivera-Galdos, M. Vockel, R. Linnepe, U. Ipe, A. Stadtmann, A. Zarbock, et al. 2014. Leukocyte extravasation and vascular permeability are each controlled in vivo by different tyrosine residues of VE-cadherin. *Nat. Immunol.* 15:223–230. http://dx.doi.org/10.1038/ni.2824

Winger, R.C., J.E. Koblinski, T. Kanda, R.M. Ransohoff, and W.A. Muller. 2014. Rapid remodeling of tight junctions during paracellular diapedesis in a human model of the blood-brain barrier. *J. Immunol.* 193:2427–2437. http://dx.doi.org/10.4049/jimmunol.1400700

Wu, Q.Y., M.R. Sun, C.L. Wu, Y. Li, J.J. Du, J.Y. Zeng, H.L. Bi, and Y.H. Sun. 2015. Activation of calcium-sensing receptor increases TRPC3/6 expression in T lymphocyte in sepsis. *Mol. Immunol.* 64:18–25. http://dx.doi.org/10.1016/j.molimm.2014.10.018

Xie, J., S.K. Cha, S.W. An, M. Kuro-O, L. Birnbaumer, and C.L. Huang. 2012. Cardioprotection by Klotho through downregulation of TRPC6 channels in the mouse heart. *Nat. Commun.* 3:1238. http://dx.doi.org/10.1038/ncomms2240

Yeh, J.C., L.A. Otte, and J.A. Frangos. 2008. Regulation of G protein-coupled receptor activities by the platelet-endothelial cell adhesion molecule, PECAM-1. *Biochemistry.* 47:9029–9039. http://dx.doi.org/10.1021/bi8003846

Yip, H., W.Y. Chan, P.C. Leung, H.Y. Kwan, C. Liu, Y. Huang, V. Michel, D.T. Yew, and X. Yao. 2004. Expression of TRPC homologs in endothelial cells and smooth muscle layers of human arteries. *Histochem. Cell Biol.* 122:553–561. http://dx.doi.org/10.1007/s00418-004-0720-y

Zhang, Y., K. Ma, P. Sadana, F. Chowdhury, S. Gaillard, F. Wang, D.P. McDonnell, T.G. Unterman, M.B. Elam, and E.A. Park. 2006. Estrogen-related receptors stimulate pyruvate dehydrogenase kinase isoform 4 gene expression. *J. Biol. Chem.* 281:39897–39906. http://dx.doi.org/10.1074/jbc.M608657200

Zhang, Z., J. Tang, S. Tikunova, J.D. Johnson, Z. Chen, N. Qin, A. Dietrich, E. Stefani, L. Birnbaumer, and M.X. Zhu. 2001. Activation of Trp3 by inositol 1,4,5-trisphosphate receptors through displacement of inhibitory calmodulin from a common binding domain. *Proc. Natl. Acad. Sci. USA.* 98:3168–3173. http://dx.doi.org/10.1073/pnas.051632698

Zitt, C., A.G. Obukhov, C. Strübing, A. Zobel, F. Kalkbrenner, A. Lückhoff, and G. Schultz. 1997. Expression of TRPC3 in Chinese hamster ovary cells results in calcium-activated cation currents not related to store depletion. *J. Cell Biol.* 138:1333–1341. http://dx.doi.org/10.1083/jcb.138.6.1333